Cloud and rain processes in a biosphere-atmosphere interaction context in the Amazon Region

M. A. F. Silva Dias,[1] S. Rutledge,[2] P. Kabat,[3] P. L. Silva Dias,[1] C. Nobre,[4] G. Fisch,[5] A. J. Dolman,[3] E. Zipser,[6] M. Garstang,[7] A. O. Manzi,[4] J. D. Fuentes,[7] H. R. Rocha,[1] J. Marengo,[4] A. Plana-Fattori,[1] L. D. A. Sá,[4] R .C. S. Alvalá,[4] M. O. Andreae,[8] P. Artaxo,[1] R. Gielow,[4] and L. Gatti[9]

[1]   This paper presents an overview of the results from the first major mesoscale atmospheric campaign of the Large-Scale Biosphere-Atmosphere Experiment in Amazonia (LBA) Program. The campaign, collocated with a Tropical Rainfall Measuring Mission (TRMM) satellite validation campaigns, was conducted in southwest Rondônia in January and February 1999 during the wet season. Highlights on the interaction between clouds, rain, and the underlying landscape through biospheric processes are presented and discussed.   *INDEX TERMS:* 0315 Atmospheric Composition and Structure: Biosphere/atmosphere interactions; 3314 Meteorology and Atmospheric Dynamics: Convective processes; 3307 Meteorology and Atmospheric Dynamics: Boundary layer processes; 3322 Meteorology and Atmospheric Dynamics: Land/atmosphere interactions; *KEYWORDS:* clouds, LBA, TRMM, biosphere, forest

1.   Introduction

[2]   The first major atmospheric mesoscale campaign in the wet season (WETAMC) of the Large-Scale Biosphere-Atmosphere Experiment in Amazonia (LBA) [*LBA*, 1996] was held in January and February 1999. The campaign was organized jointly with the Tropical Rainfall Measuring Mission (TRMM) validation campaign (known as TRMM/LBA). Both campaigns took place in southwest Amazon basin in the Brazilian state of Rondônia (see Figure 1).

[3]   The major objectives of the WETAMC field campaign were:

1. to understand the coupling between biosphere and atmosphere processes in the wet season in the Amazon region including budgets of heat, water vapor, CO_2, trace gases and volatile organic compounds (VOC);

2. to determine the cloud dynamics and microphysics interactions over rain forest and over adjacent deforested areas including the role of anthropogenic and biogenic aerosol particles as cloud condensation nuclei (CCN);

3. to understand the local response of clouds and rainfall to large-scale forcing;

4. to improve modeling of biosphere-atmosphere processes in different scales.

[4]   The major objectives of TRMM/LBA included:

1. to validate the kinematic, microphysical and diabatic heating fields obtained by the TRMM satellite in the context of tropical continental convection;

2. to validate TRMM satellite algorithms in the context of tropical continental convection.

[5]   The objective of this paper is to present the several findings based on the field campaign results that are related to the above listing of a broader scope project. Mainly, the link between cloud processes (microphysics and thermodynamics) and the surface processes (including the surface fluxes) will be addressed here. The behavior of trace gases, VOCs and their impact on atmospheric chemistry and eventually on aerosol and CCN are presented in a companion paper by *Andreae et al.* [2002].

[6]   The preliminary results of data analysis of the WETAMC/LBA and TRMM/LBA indicate a picture of an intrinsically coupled rain producing system where different surface and atmosphere processes interact at different space and timescales, from the local to the large scale, and from a few hours to several days, respectively. The details of each process involved are presented in more focused way in several papers of this issue. Here we aim at presenting an integrated picture of the first results, highlighting the main scientific questions that arise as

[1]Departmento de Ciêcias Atmosféricas, Universidade de São Paulo, São Paulo, Brazil.

[2]Department of Atmospheric Sciences, Colorado State University, Fort Collins, Colorado, USA.

[3]Alterra, Wageningen, Netherlands.

[4]Centro de Previsão de Tempo e Estudos Climáticos, Instituto Nacional de Pesquisas Espaciais, Brazil.

[5]Instituto de Atividades Espaciais, Centro Tecnológico da Aeronáutica, São José dos Campos, Brazil.

[6]Department of Meteorology, University of Utah, Salt Lake City, Utah, USA.

[7]Department of Environmental Sciences, University of Virginia, Charlottesville, Virginia, USA.

[8]Max Plank Institute for Chemistry, Mainz, Germany.

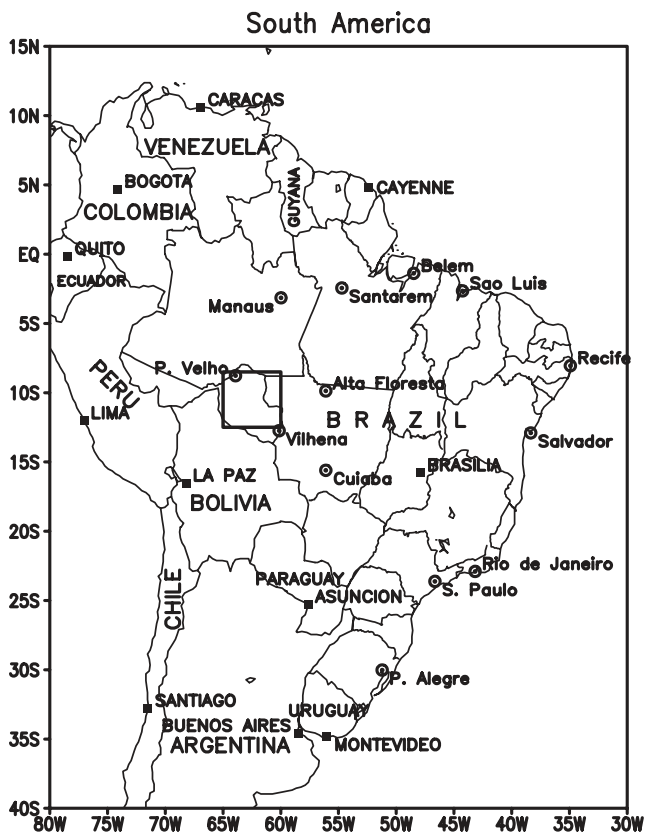[9]Instituto de Pesquisas Energéticas e Nucleares, São Paulo, Brazil.

Figure 1. Map of South America. The square denotes the experimental area in the state of Rondônia.

we begin to unravel the mysteries of rainfall generation in this region.

2. Experimental Setup and Observations

[7] The complete set of equipment involved in the WETAMC/LBA and TRMM/LBA experimental design were the following (see Figure 2 for locations):

1. radiosonde sites performing 6–8 soundings per day, located at Rebio Jaru, Rancho Grande, ABRACOS (Anglo-Brazilian Amazonian Climate Observation Study site [*Gash et al.*, 1996]) pasture and Rolim de Moura;

2. tethered balloon sites for boundary layer meteorology; located at Rebio Jaru, ABRACOS pasture and Rolim de Moura;

3. forest (at Rebio Jaru) 60 m micrometeorological tower instrumented with 3 levels of eddy covariance measurements and vertical profiles of radiation, temperature, humidity and wind speed;

4. forest (at Rebio Jaru) 54 m tower instrumented for atmospheric chemistry measurements, including carbon dioxide (CO_2), nitrous oxides (NO_x), ozone O_3 and aerosol;

5. forest (Rebio Jaru) and pasture (ABRACOS) arrays for soil temperature and soil moisture and set of rings for soil respiration;

6. pasture towers (ABRACOS and Rolim de Moura) with temperature, humidity and wind profiles, and eddy correlation measurements including heat, moisture and CO_2 flux;

7. pasture tower (ABRACOS) for atmospheric chemistry measurements, including CO_2, NO_x, O_3, aerosol, and spectral radiation measurements;

8. wind profiler sodars (ABRACOS and Rolim de Moura), 1 with radio acoustic sounding system (RASS) (Rolim de Moura);

9. complete automatic weather stations (Rebio Jaru, Rolim de Moura, ABRACOS pasture);

10. lightning detection network deployed by NASA/ Marshall Space Flight Center;

11. Four rain gauge networks with a total of 40 gauges (networks in Figure 3) and 4 disdrometers (Ji-Paraná, ABRACOS Hill) deployed and operated by NASA TRMM Office and the University of Iowa;

12. Doppler radars: the NCAR S-POL (at Fazenda Jamaica, includes full polarimetric capabilities at S-band) and the TOGA C-band radar (at ABRACOS Hill), radar coverage in Figure 3;

13. dual-wavelength radar profiler operated by the NOAA Aeronomy Laboratory (at Ji-Paraná);

14. Aircraft: University of North Dakota Citation II for in-situ sampling of microphysical variables and the NASA ER-2 carrying the EDOP radar (ER-2 Doppler, X band radar) used to provide high resolution data on cloud vertical velocity and reflectivity structures, and AMPR (Airborne Microwave Profiling Radiometer), a multifrequency radiometer similar to the TMI instrument on TRMM.

[8] The period of observation varies somewhat according to the observation platform but a more complete set of observations is available for the period from 20 January to 24 February 1999. Most of the data has been processed and gone through a first level of quality control. Besides the equipment installed in Rondônia, a special upper-air observations network was installed since April 1997 as part of a program to improve the understanding of climate variability

Figure 2. WETAMC/LBA and TRMM/LBA sites. Shaded in the background is topography with light gray denoting higher terrain. See color version of this figure at back of this issue.
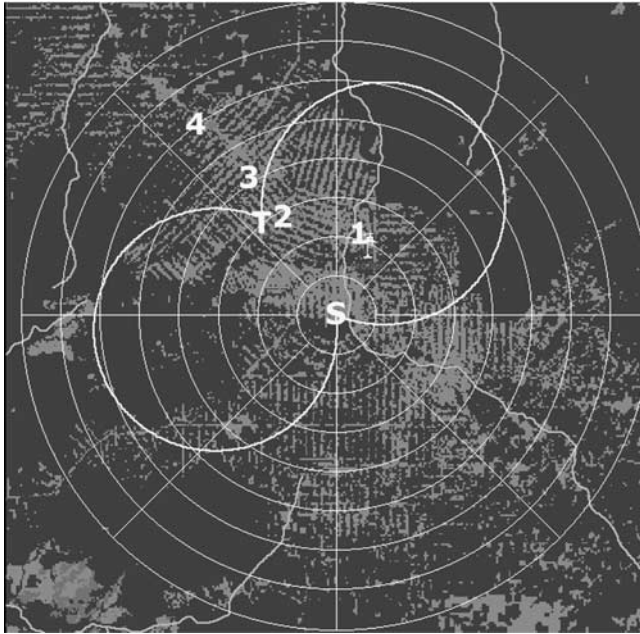
Figure 3. Deforestation in the background in light green. Dark green is forest. Rain gauge networks in red. Center of the range circles (at every 20 km) is at the S-Pol position in Fazenda Jamaica. Yellow circles are the Dual Doppler regions. TOGA radar position is indicated by T. S-Pol position is indicated by S. Rain gauge networks are indicated by numbers 1, 2, 3, and 4. See color version of this figure at back of this issue.

over the eastern Pacific and South America [*Douglas and Peña*, 2000].

[9]   During late 1998 funding became available from the NASA-LBA Hydrometeorology Program to reestablish atmospheric sounding sites in eastern Bolivia as part of the Brazil-based TRMM/LBA and WETAMC/LBA. The network that finally evolved consisted of one radiosonde station in Santa Cruz and 4 pilot balloon sites elsewhere in Bolivia [*Marengo et al.*, 2002]. The complete discussion of each observing platform and its performance may be found in the individual papers in this issue.

[10]   The operational weather data of South America has been incorporated into the WETAMC data set as well as the global analysis from CPTEC/NCEP and the ECMWF. During the field campaign an operational mesoscale weather forecast using the Regional Atmospheric Modeling System (RAMS) with the global CPTEC forecast as boundary conditions was used to help the planning of the daily aircraft operations. After the campaign, RAMS has been used [*Silva Dias et al.*, 2000] in a downscaling mode to obtain a mesoscale analysis with 20 km resolution incorporating the surface observations from the operational networks and from the WETAMC sites. For the special cases, higher resolution simulations have been performed [see *Silva Dias et al.*, 2002] using the WETAMC radiosonde observations incorporated in the initial conditions.

3.   Summary of Previous Work

[11]   The behavior of clouds and precipitation in the Amazon region was first studied during the Amazon Boun-

dary Layer Experiment (ABLE 2A and 2B) during the years of 1985 and 1987, respectively (see *Harris et al.*, 1988 and *Harris et al.*, 1990, respectively). *Greco et al.* [1990] described the convective systems in different scales as the Coastal Occurring Systems (COS), Basin Occurring Systems (BOS) and Local Occurring Systems (LOS) in decreasing length and lifetimescales. The COS has received more attention [*Garstang et al.*, 1994; *Greco et al.*, 1994; *Silva Dias and Ferreira*, 1992; *Cohen et al.*, 1995] being a squall line which is characterized by its longevity, frequently more than 1 day, and its length of hundreds of km, frequently reaching 1,000 km. COS propagate due south and west starting at the Northern Coast of South America and reaching the southwest Amazon, being observed all year-round but being more frequent during August and September, the dry season [*Cohen et al.*, 1989; *Silva Dias*, 1999]. A direct link between cloud development and land features was not addressed at that time, nor an analysis of the microphysics of clouds.

[12]   Several studies have addressed the impact of tropical convective heat sources on the large-scale circulation. *Silva Dias et al.* [1983] have shown that there is a strong coupling between the tropical heat source in Amazon and the upper level cyclonic circulation known as the Bolivian High. *Grimm and Silva Dias* [1995] and *Gandú and Silva Dias* [1998] show that the tropical heat source over the Amazon and its extension toward the southeast, known as the South Atlantic Convergence Zone (SACZ), are coupled to other tropical heat sources (mainly the South Pacific Convergence Zone and the African heat source and the associated South Indian Convergence Zone) so that perturbations imposed in one will affect the others at a timescale of intraseasonal oscillations, in the 20–60 day range. Conversely, the impact of the large-scale circulation on convection has been addressed from the point of view of seasonal differences between the dry and the wet season [e.g., *Horel et al.*, 1989].

[13]   The effects of deforestation on precipitation in the Amazon have been addressed in modeling studies. *Nobre et al.* [1991] showed that a complete change of vegetation from forest to pasture in the Amazon Basin would lead to an increase of surface temperature and a decrease in precipitation. However, the Amazon is being deforested gradually and in specific patterns as the one seen in Figure 3 for the state of Rondônia where deforestation is observed around the main roads in geometrical patterns (the so-called *fish bone* deforestation). Most of the results have focused on the dry season effects of deforestation. *Cutrim et al.* [1995] showed that shallow cumulus form over deforested areas in the dry season as well as over elevated terrain. *Silva Dias and Regnier* [1996] and *Souza et al.* [2000] have shown that local circulations develop during the dry season from forest to pasture enhancing low level convergence. *Fisch et al.* [1996] showed also in the dry season that the maximum mixed layer over pasture was several hundred meters higher than over forest. Forests in the Amazon have an evapotranspiration behavior that is almost aseasonal [*Wright et al.*, 1992; *Maia Alves et al.*, 1999] while pasture has a strong seasonal cycle so that differences between wet and dry season would be expected mainly for deforested areas. *Wang et al.* [2000] numerically simulated the impact of deforestation on rainfall during wet, dry and transition seasons in Rondônia. He found a negligible impact of

deforestation on rainfall in the wet season although his main focus was in very wet periods.

[14] From the above summary it is seen that there are gaps in the understanding of moist convection in the Amazon and its interaction with the surface and with the large-scale circulation. The LBA, and more specifically, the WETAMC/LBA and the TRMM/LBA campaign preliminary results address some of this gaps.

4. Results

[15] Significant stratiform precipitation has been identified during the early phase of the experiment, dominated by the presence of the SACZ. *Herdies et al.* [2002] show that a bimodal pattern prevails in low level winds with successive periods of easterlies and westerlies while *Rickenbach et al.* [2002] and Laurent show that the wind regimes are associated with changes in cloud features as will be described further on. The average rainfall in the ABRACOS rain gauge for January was 266 mm and for February 468 mm [*Tota et al.*, 2000]. The several networks defined in Figure 3, net1, net2, net3, and net4, measured for January, 283.1, 349.2, 179.2 and 252.6 mm, and for February, 182.0, 158.3, 147.7 and 232.4 mm, respectively.

4.1. The Large-Scale Variability During January and February

[16] The 3 rainiest months in the Amazon basin vary from December–January–February in the southern area, including Rondônia, to April–May–June in the northern portion of the basin. Along the central part of the basin the 3 rainiest months vary from February–March–April in the east to March–April–May in the west [*Rao and Hada*, 1990]. The Amazon rainfall regime is influenced by the El Niño/Southern Oscillation (ENSO) phenomena and the eastern portion of the basin is particularly influenced by ENSO [e.g., *Bell et al.*, 1999]. Nevertheless, the WETAMC/LBA campaign took place during the transition from the warm to the cold phase of ENSO and the rainfall anomaly, during this period, was not particularly related to the standard ENSO pattern. Figure 4 shows the precipitation anomaly with respect to a 30 year average observed in January and February 1999. It is worthwhile pointing out the east/west gradient of the precipitation anomaly, with significantly dry anomaly to the east, both in January and February (below 100% of the normal for northern Central Brazil). Possible feedbacks of the east/west precipitation anomaly in the regional circulation may be expected in view of the impact in the soil moisture content and surface energy exchange.

[17] The time variability of the rainfall over large areas in the tropics is modulated by intraseasonal variability in the 20–60 day range [*Kousky and Kayano*, 1994; *Madden and Julian*, 1994; *Kayano and Kousky*, 1998]. Most of the intraseasonal signal is associated with an eastward propagating wave with maximum activity in the equatorial region. Figure 5 shows a composite of the outgoing longwave radiation (OLR) during the Southern Hemisphere summer months (a proxy to tropical precipitation) in timescales of −24, −14, −4, 6 and 16 days lag in reference to maximum precipitation at lag −4 in the SACZ region over SE Brazil. The composite shown in Figure 5 is based on 14 summers (1981 to 1995). Alternating dry and wet conditions separated by about 20–30 days prevail over the SACZ
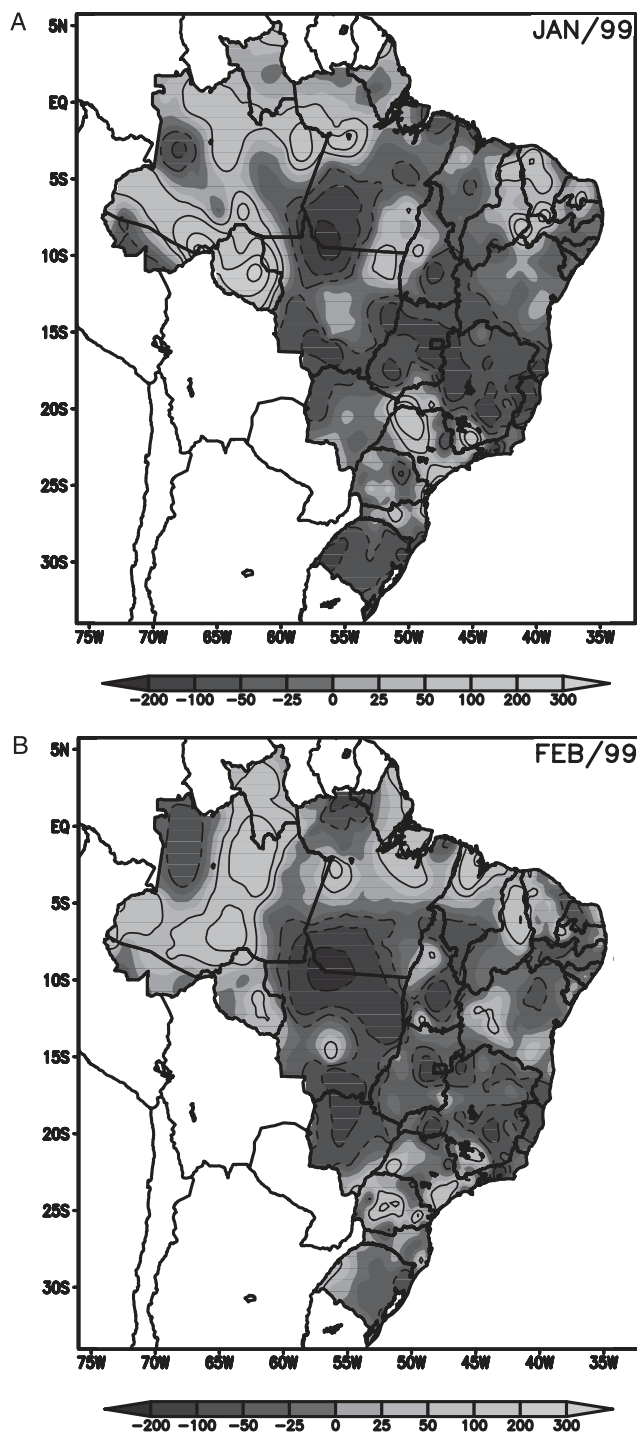
Figure 4. Precipitation anomaly for January and February 1999, from the operational Brazilian network. Prepared by CPTEC/INPE.

region, associated to major changes in the low and upper level circulation [*Nogues-Paegle and Mo*, 1997] affecting most of tropical South America.

[18] The intraseasonal variability of the SACZ is seen locally in Rondônia in the wet season as a variable low level wind regime. Figure 6 shows the zonal wind component at 700 hPa from the NCEP analysis at a grid point in central Rondônia. The zonal wind oscillations depicted in Figure 6 are coherent with the expected impact of the intraseasonal
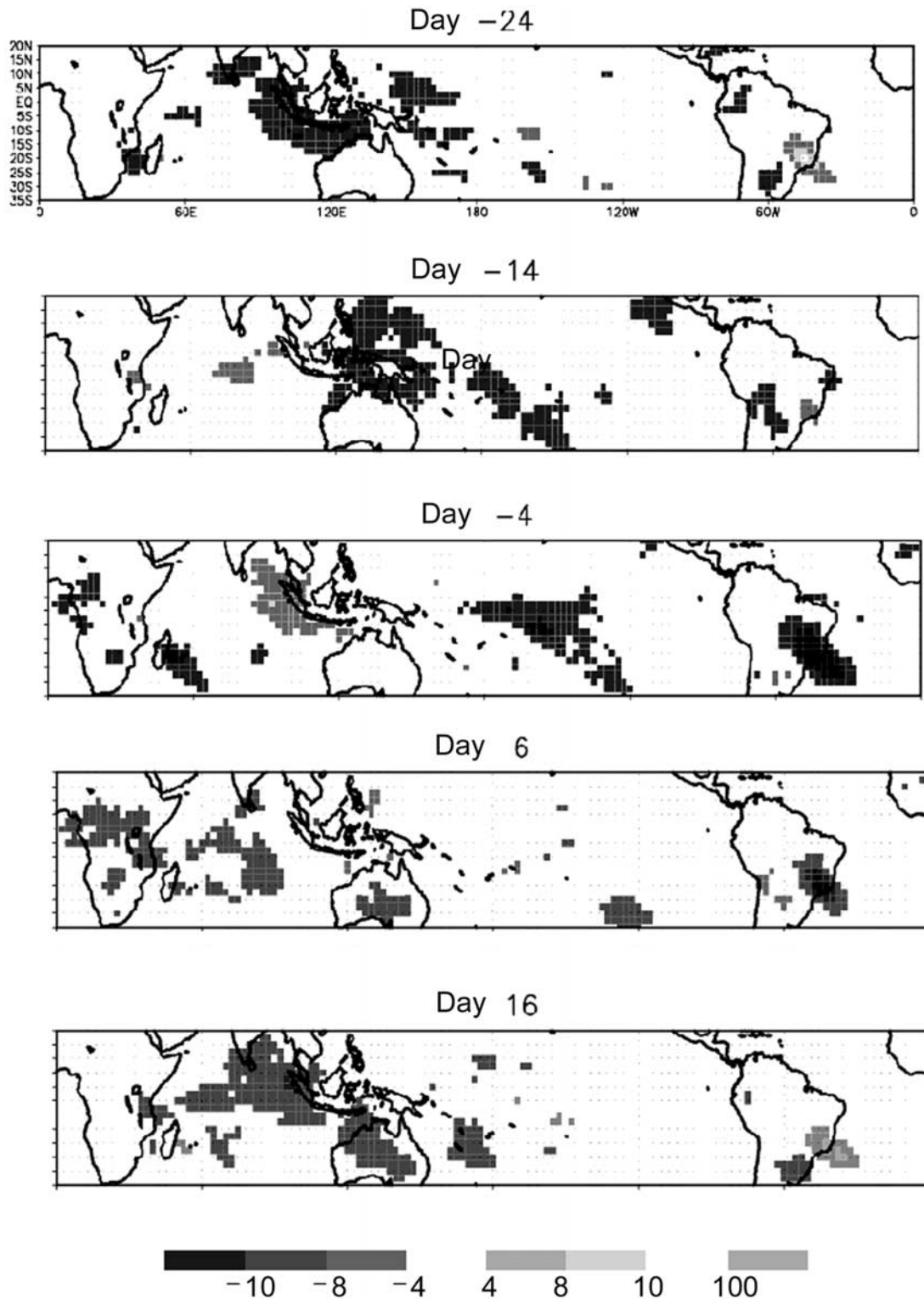
Figure 5. OLR anomaly composites with respect of to the day of minimum OLR in southeast Brazil [from *Marton and Silva Dias*, 2001].

oscillations as discussed at length by *Marton and Silva Dias* [2001], *Carvalho et al.* [2002], and *Herdies et al.* [2002].

4.2. Clouds and Rain in Amazônia

[19] One of the striking features of clouds in the Amazon has been summarized by *Petersen and Rutledge* [2001]

using data from the precipitation radar aboard the TRMM satellite. Frequencies in the 30–35 dBz range show high values in the 7–10 km region for clouds in the Congo and in N. Australia but low values for the W. Pacific and the Amazon region. *Pertersen and Rutledge* [2001] have discussed the association of these values to the ice water
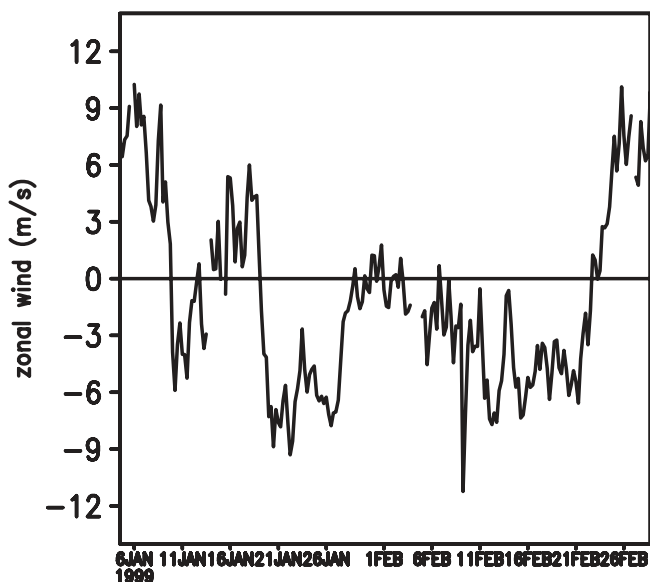
Figure 6. Zonal wind component from NCEP global analysis at 700 hPa at a grid point close to the center of Rondônia (11°S, 62°W) for January and February 1999.

content and showed a direct relationship of the ice water content to the frequency of lightning. *Zipser and Lutz* [1994] indicate as a necessary condition for rapid electrification, that a convective cell must have its updraft speed exceed some threshold value. Based upon field program data in tropics and mid latitudes, they made a tentative estimate for the magnitude of this threshold of 6–7 m s^{-1} for mean speed and 10–12 m s^{-1} for peak speed. *Mohr and Zipser* [1996] and *Mohr et al.* [1999] noted that the Amazon region has an apparently weaker population of convective storms than tropical Africa, using ice scattering signatures from the Special Sensor Microwave Imager (SSM/I), with the frequency distribution of apparent intensity similar to that of oceanic convective systems. The similarity of the Amazon features with maritime features and different from the more continental ones in the tropics, has prompted the use of the term ''green ocean'' with reference to the Amazon. *Petersen et al.* [2000] have also shown that during the rainy season in the Amazon lightning goes through a succession of maxima and minima. *Rickenbach et al.* [2002] focus on the convective fractional area in the cloud systems observed by the TOGA radar and show that when the convective fraction is large, the low level winds are from the east while when the convective fraction is low, i.e., the stratiform area is larger, the low level winds are from the west. *Laurent et al.* [2002] show based on GOES images and TOGA radar data that during the easterly regime, upper level cloudiness and rain cells are seen to propagate due west while in the westerly regime there is a slight tendency for rain cells to move due east while the upper level cloudiness propagates independently. *Anagnostou and Morales* [2002] compare the two regimes and show that the easterly regime has higher mean rainfall because of higher convective rainfall intensities while stratiform rainfall is about the same for both regimes. *Carvalho et al.* [2002] analyzing infrared satellite images for the same period, also show that clouds properties are modulated by

the low level wind regime in that in the easterly regime the number of systems active at any time is lower than in the westerly regime but the fraction of cold tops is larger for the easterly regime. *Tokai et al.* [2002] show from disdrometer data at the surface, that raindrop radius reach larger values in the easterly regime than in the westerly regime. *Carey et al.* [2001] use the S-Pol radar data and show that consistent with more vertically developed and intense convection, the easterly regime clouds exhibit higher reflectivities, drop diameters and rain rates then westerly regime clouds.

[20] Figure 7 shows the typical wind flow at 700 hPa over the Amazon Basin during the easterly and the westerly phases. Note that the wind shifts in the southern half of the region from easterly to westerly while in the northern half it shows a shift from east to a more northerly component. *Williams et al.* [2002] looking at cloud condensation nuclei (CCN) concentration throughout the rainy season show the CCN concentrations are lower in the westerly regime at about 400 cm^{-3} while in the easterly regime they are as an average about 800 cm^{-3}. As a reference, during the dry season, CCN concentrations increase up to about 2000–3000 cm^{-3} as a result of biomass burning.

[21] *Williams et al.* [2002] mention that during the transition from the dry to the wet seasons in Rondônia,
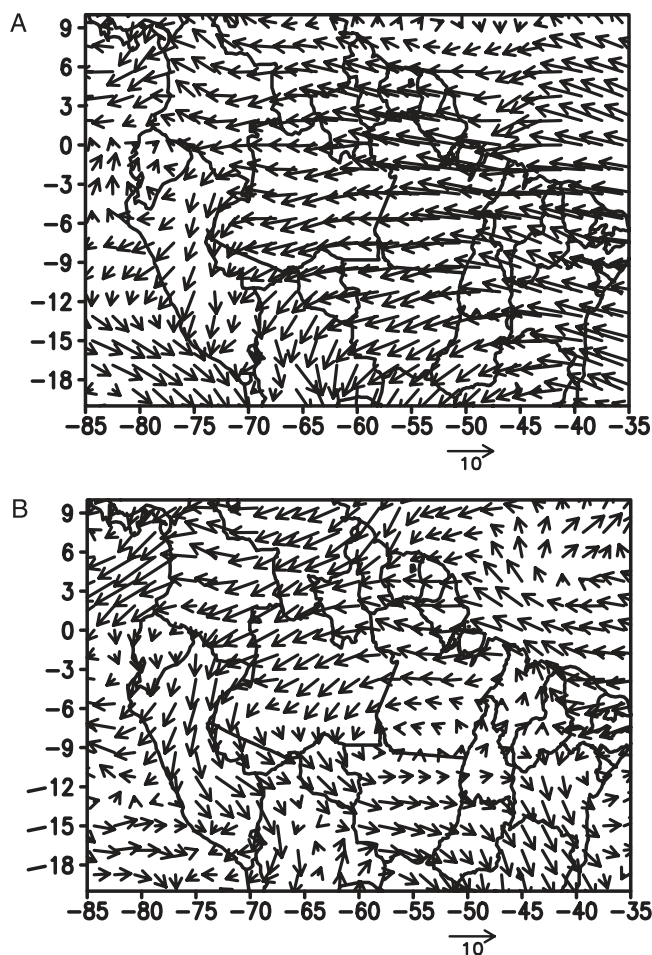
Figure 7. Wind field at 700 hPa from the NCEP global analysis for typical days: 15 February 1999, an easterly case for southwest Amazon, and 24 February 1999, a westerly case.

convective systems are very continental with towering tops reaching maximum heights of up to 19–20 km. However, even after the atmosphere becomes cleaner, following several events of significant rainfall, the systems are still very continental, revealing limitations to the dominant role of the CCN concentration. *Rosenfeld* [1999], on the other hand, shows evidence, based on the TRMM radar data, that smoke-laden tropical clouds have to grow beyond the −10°C isotherm to precipitate, indicating suppression of the warm rain processes based on collision and coalescence.

[22] The sources of CCN in the Amazon region during the wet season are complex and still not fully understood. *Formenti et al.* [2001] and *Artaxo et al.* [2002] have investigated the composition of aerosol during the wet season in the Amazon. Measurements performed at about 1000 km from the northern coast of So. America at Balbina and Santarem show a significant component of Saharan dust with addition of sea salt and marine biogenic sulfates. Other significant components come from biogenic sources such as primary biogenic particles and the emission of volatile organic compounds (VOC) and sulfur gases. Conversion of gaseous precursors to substances of low volatility and their deposition on preexisting particles provides them with enough soluble material to be able to act as CCN.

[23] The aerosols during the wet season at the Northern coast of South America are of maritime and biogenic origin while in Rondônia they are basically of biogenic origin [*Artaxo et al.*, 2002]. In the Southwestern Amazon, the distance to the northern and to the eastern coast of South America is more than 3000 km. During the rainy season, the incoming air masses from the north or east, in either wind regime will go through several cloud cycles and most of the maritime species will rain out or wash out of the equatorial air mass. *Roberts et al.* [2001] argue that convective clouds provide a source of newly nucleated particles at cloud top. These are not CCN at the start; however, sulfates and soluble organics deposit on these particles, which are then easily activated into CCN. The exchange of trace gases and aerosols between the rain forest and the atmosphere is presented in more detail by *Andreae et al.* [2002] and a series of detailed papers on the results of the LBA-EUSTACH program.

[24] The basic picture that puts together all the above features in the different wind regimes is based on two modes of convection. During the easterly regime, convective systems are more continental, with vigorous convective cells, more isolated, with a well define mixed ice water region and frequent lightning. During the westerly regime, the systems are larger and more stratiform, with no mixed ice water phase region and almost no lightning. *Cifelli et al.* [2002] describe the 26 January 1999 (easterly phase) and 25 February (westerly phase) cases in detail, providing further documentation on the distinct differences seen between convective systems in the easterly and westerly phases. To incorporate the role of CCN into this picture involves looking also into the dynamic/thermodynamic forcing provided by different regimes.

[25] The evolving picture may be seen as an interrelation of processes at different scales. Starting from a large-scale forcing, in an intraseasonal timescale, in the form of a low level westerly regime which is associated with low level convergence and absence of convective inhibition, rain starts to pick up, from a more convective type to gradually more stratiform with weaker convection and weaker convective updrafts. As CCN become less available, warm rain processes dominate, lightning is basically absent and precipitation has moderate maximum in the afternoon (cf. section 4.3). As the large-scale forcing changes to an easterly regime, with no large-scale associated low level convergence, clouds start to respond to daytime heating and to surface heterogeneities, becoming more localized. Biogenic CCN become more abundant since there is less chance to be entrained and scavenged in a cloud updraft. The increased amount of CCN happens simultaneous to an increase in convective activity and convective updrafts; anyway, the warm rain process are inhibited and the ice water mixed phase region becomes more prominent and lightning is observed. Larger raindrops are observed at the surface in the easterly regime because they are formed by melting graupel that went through considerable growth by collection of water drops and ice crystals.

[26] A stronger than normal thermal inversion typical of the transition from dry to wet season may inhibit cloud formation in such a way than only very few clouds are formed and those that do form need very strong updraft to overcome the thermodynamic convective inhibition. In this case, even if the atmosphere has low CCN concentration, the enhanced updrafts would not allow time for the warm rain coalescence process to take place.

[27] The conceptual model described above, although internally consistent, has several hidden questions and unknowns that need further research. The transition from one phase to another has to be better understood, the time involved in recovering the CCN concentration, the role of CCN concentration and the details of the evolution from one mode of convection to the other are still unknown. However, it is apparent that the primary forcing for the different convective modes is the large-scale dynamics and thermodynamics while the evolution of the CCN is closely related to these.

[28] The remote and regional impacts of the two basic modes of convection can be quite different in view of the vertical structure of the associated heat sources. The vertical profile of the heat source is expected to peak up at the mid to upper troposphere in the highly convective regime (low level easterly flow) while a maximum heating at the lower troposphere is associated with the weaker convection and more stratiform regime (low level westerly flow). A stronger remote response is favored by the deep heating according to *DeMaria* [1985]; low level heating leads to a more confined tropospheric response. The level of maximum convective heating rate is produced in numerical models by the convective parameterization which is usually biased to deep convection. Further research into the convective parameterizations of Amazonian convection in the wet season in global models is necessary to ensure that global climate impacts of changes in the Amazon region will be adequately modeled.

4.3. The Diurnal Cycle

[29] *Betts et al.* [2002a] discuss the surface diurnal cycles of temperature, humidity, lifting condensation level, equivalent potential temperature and the surface fluxes for easterly and westerly regimes in the ABRACOS site (cf. Figure 2). They show that the downward solar radiation

and the fluxes of sensible and latent heat are lower for the westerly regime and that the water vapor mixing ration is higher but with a weaker diurnal cycle. The easterly regime shows an early morning maximum of mixing ratio followed by a fall to a minimum in the late afternoon as the cumulus clouds mix water vapor up and out of the subcloud layer in a higher rate than the one provided by surface evaporation. They also show that there is a steady transition throughout January and February 1999 toward cloudier conditions and lower surface fluxes. *Betts and Jacobs* [2002] compare the mean diurnal cycle of the same variables to the ECMWF short term forecasts and show that the model produces precipitation 2 hours after sunrise and several hours earlier than observed. The surface thermodynamic variables in the model have a diurnal cycle which is quite close to that observed but this is produced in the model by a different mix of boundary layer and surface processes, more rainfall evaporation and less shallow cumulus convection than generally observed, similar to the westerly regime seen in late February. *Betts et al.* [2002a] suggest that the way several models treat convection in two separate subroutines, one for shallow and another for deep convection may not be the more adequate solution in view of the results obtained.

[30] *Machado et al.* [2002], *Negri et al.* [2002], and *Anagnostou and Morales* [2002] examine the diurnal cycle of convection as seen by GOES and/or TRMM satellite sensors, by the TOGA radar and by the rain gauge network. The rain gauge network data show clearly a preference for maximum rainfall intensity between 1200 and 1600 LST while in some periods, a second maximum shows up between 0000 and 0400 LST [*Tota et al.*, 2000]. *Anagnostou and Morales* [2002] indicate that the diurnal peak of the easterly flow regime is about one hour later than in the westerly regime. *Machado et al.* [2002] show that for the WETAMC area shown in Figure 1, the minimum cloud cover occurs only a few hours before the maximum precipitation and the maximum cloud cover occurs at night. The maximum rainfall takes place at the time of maximum initiation of the convective cells observed by satellite and rain cells observed by radar. *Negri et al.* [2002] analyze a larger area encompassing the whole Amazon Basin and examine the effect of geography (rives, lakes, coasts) and topography on the diurnal cycle. Rainfall is seen to avoid the Amazon river in the afternoon while an early morning maximum is seen over the large rivers.

[31] High temporal resolution tropospheric ozone data for the tropics are scarce. Thus, to investigate how ambient ozone levels vary with time of day at the pasture site near Ji-Paraná, hourly averages were determined for all days during January to February 1999. Ozone mixing ratios exhibited strong diurnal variations. Rapid increases were observed from sunrise until local noon in response to both vertical transport of ozone-rich air from aloft to the surface and local photochemical production. Averages of peak ozone levels reached ~20 ppb and occurred during 1400 and 1500 h (Figure 8a), reflecting the time of intense local photochemical activity. During the night the stable boundary layer uncoupled the surface from the atmosphere above. As a result, the ozone within the nocturnal stable boundary layer (100–200 m indepth) progressively declined after sunset due to the effective deposition to the grass surface (J. M. Sigler et al., Ozone dynamics and deposition processes at a deforested site in the
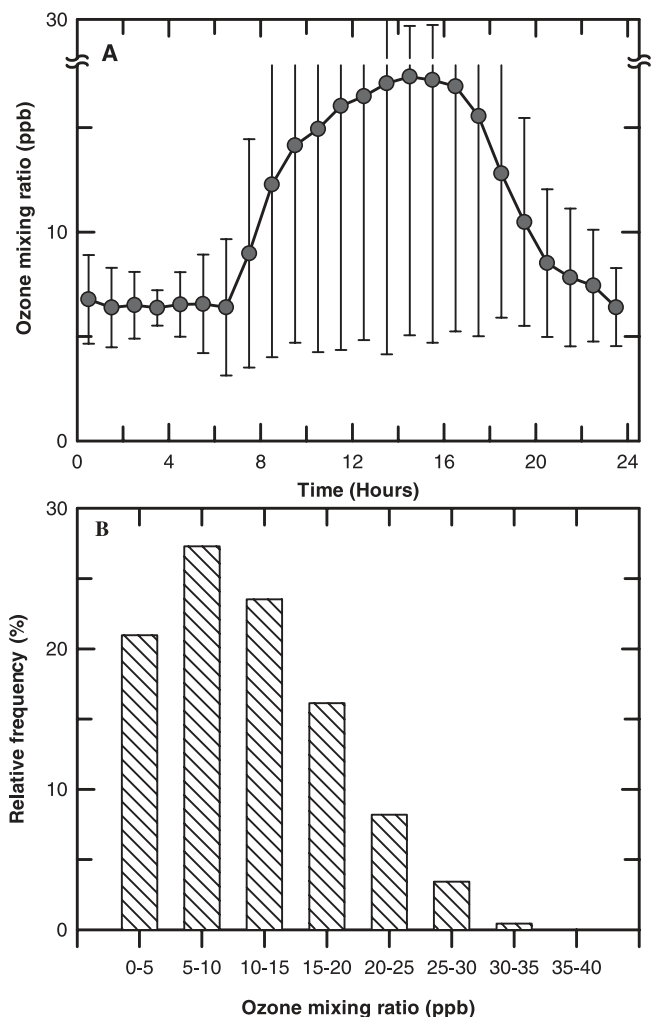

Figure 8. (a) Composited diurnal ozone mixing ratios measured at the pasture site in Rondônia during the wet season months of January and February 1999. The vertical bars denote standard deviations. (b) Relative frequency (in %) estimated for the ambient ozone levels during the measurement period.

Amazon basin, submitted to *Ambio*, 2000, hereinafter referred to as Sigler et al., submitted manuscript, 2000) and reaction of ozone with nitric oxide. On average, nighttime ozone levels reached minimum values of ~5 ppb, just before sunrise. Compared to ozone measured over forests at Central Amazon during the wet season, ozone levels over the deforested site of this study were higher: to 20–45 ppb over the deforested field while *Kirchhoff et al.* [1990] show 6–10 ppb at 15 m above a Central Amazon forest. In part, these differences in ozone dynamics are due to photochemical and surface deposition processes. At the pasture site, the most prevailing ambient ozone levels during the wet season were within 5–10 ppb, with a frequency of more than 25% (Figure 8b). The ozone dynamics at the pasture site during the dry season is discussed by *Kirkman et al.* [2002].

4.4. The Effect of Convective Storms on Boundary Layer Ozone

[32] The effect of convective storms in Rondônia on boundary layer O_3 is analyzed by *Betts et al.* [2002b]. This
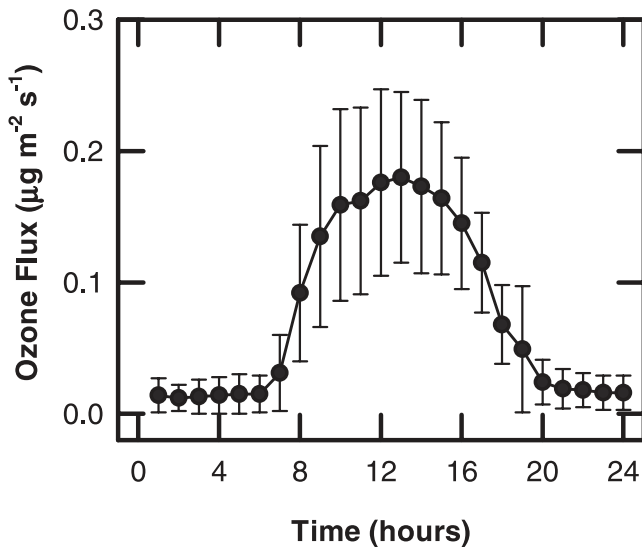
Figure 9. Equivalent potential temperature and ozone (inverted scale on the right) for the ABRACOS site, from *Betts et al.* [2002a, 2002b], for 17–18 February 1999.

effect is more visible at night when O_3 values are low in the nocturnal stable surface (Figure 8a). However, O_3 concentrations increase with height [*Gregory et al.*, 1988] so that a well organized convective system with well defined downdrafts may bring higher values of O_3 to the surface. Equivalent potential temperature (θ_E) is a known tracer for downdrafts [*Zipser*, 1969, 1977] so that a comparison of θ_E with O_3 concentration provides a means of interpretation of convective impact; Figure 9, from *Betts et al.* [2002b], shows an example of a plot of θ_E and O_3 during the night of 17–18 February 1999 associated with nocturnal storms of the COS type as defined by *Greco et al.* [1990]. The close coupling of variations of these two variables in short timescales, which are negatively correlated so that low values of θ_E are associated with high values of O_3, is indicative of the transport of ozone by convective downdrafts. The impact of convective storms on the surface ozone budget requires further research as well as its effect on vegetation processes that feed back to the atmosphere.

4.5. Local Effects of Deforestation on Soil Temperature and Moisture and on Surface Fluxes

[33] Soil moisture and temperature are important growth factors, regulating processes in the soil-plant-continuum. Soil temperature depends on the soil heat flux [*van Wijk*, 1963], which is an important parameter in plant growth-energy balance models, as well as in meteorological models [*Braud et al.*, 1995]. Soil moisture and temperature profiles and soil heat fluxes were therefore measured within the

Table 2. Energy Budget Averaged Over 12 Days Between 6 February and 1 March[a]

Site	Rn	LE	H
FNS pasture	130.2	98.3	31.8
JARU forest	140.0	116.1	22.8
JARU-FNS	9.8	17.8	−9.0

[a]Units are in W m^{-2}, where Rn is net all wave radiation, LE is latent heat flux and H is sensible heat flux (LE was computed from the residual term of the balance between Rn and sum of H and the storage energy terms into the soil and vegetation).

WETAMC/LBA program in the forest (Reserva Jaru) and in the pasture (Fazenda Nossa Senhora-ABRACOS) sites in Rondônia during 1999 as described by *Alvalá et al.* [2002]. The wet season results show that the heat flux into the soil generally reaches up to 10 W m^{-2} and 50 W m^{-2} in the forest and the pasture, respectively, except for some peaks which are related to stronger solar forcing, such as those due to sunspecks in the forest. Measurements of temperature profiles in the soil (at depths of 2, 10, 20 and 40 cm at both sites) indicated a smaller diurnal range in the forest. The surface soil layer in the forest was always drier than in the deeper layers, because the soil is very sandy (more than 80%), which causes a fast drainage of the water after rainfall. The computed soil heat capacity for the layer 10 to 40 cm, considering the soil moisture for period between day 48 to 69 (Julian day), varied between 1.95 and 2.23 M J m^{-3} K^{-1} for the forest, and between 2.22 and 2.52 M J m^{-3} K^{-1} for the pasture. These values increase rapidly after rainfall, and decrease immediately thereafter. They are, on average, 13% higher in the pasture during the period considered. Finally, the computed apparent soil thermal diffusivity and conductivity show a behavior similar to the one presented by the soil heat capacity [*Alvalá et al.*, 2002].

[34] Table 1 shows that net all wave radiation is larger at the forest compared to the pasture because of the smaller albedo and larger net long wave radiation loss of the forest. The lower incoming solar radiation reaching the forest also suggests a more cloudy atmosphere. This is consistent with the larger incoming long wave radiation. The higher surface air temperature and humidity over the forest is consistent with the incoming and emitted long wave radiation.

[35] The energy budget (Table 2) shows the dominant role of net radiation (Rn) in latent heat flux at both pasture and forest, whose mean Bowen ratio (rate between sensible heat flux, H and latent heat flux, LE) is 0.32 and 0.20, respectively. However, the evapotranspiration of the forest was about 0.6 mm day^{-1} larger than that of the pasture, explained by the higher Rn and smaller H, which contribute with about half of this difference in the evapotranspiration.

[36] The daily cycle of the energy budget at the pasture and forest (Figure 10) shows differences between morning

Table 1. Surface Solar and Terrestrial Radiation During 30 Days Between 6 February and 11 March[a]

Site	Rn	S↓	S↑	L↓	L↑	Ln	T_a	e_w	Albedo
FNS pasture	123.0	190.0	37.7	418.9	448.2	−29.3	24.4	27.9	19.8
JARU forest	134.7	183.3	25.0	431.1	454.5	−23.4	25.9	29.6	13.6
JARU-FNS	11.7	−6.7	−12.7	12.2	6.3	5.90	1.5	1.7	−6.2

[a]Units are in W m^{-2}, except for temperature in °C, albedo in %, where Rn is net all wave radiation, S↓ is incoming solar radiation, S↑ is reflected solar radiation; L↓ is incoming long wave radiation; L↑ is emitted surface long wave radiation, Ln is net long wave radiation and Albedo is the rate between reflected and incoming solar radiation.
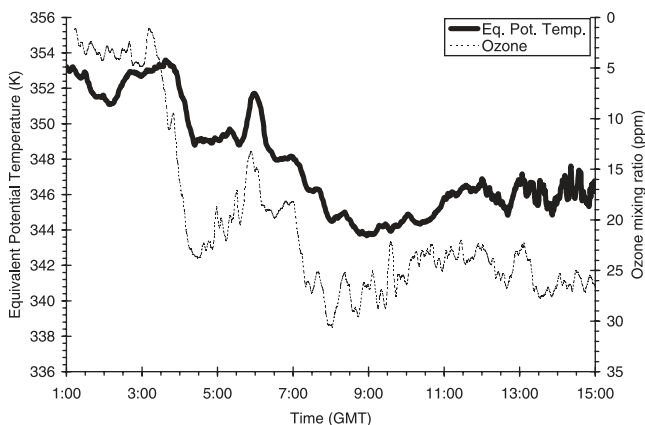
Figure 10. 12-day mean daily evolution of Rn, LE, and H for pasture (empty symbol) and forest (full symbol) between 6 February and 1 March 1999.

and afternoon behavior. Rn is larger at the forest in the morning and larger in the pasture in the afternoon. This may be explained by having cloudier skies over the forest in the afternoon. It also suggests lower cloud base in the morning over the forest since LE is always larger at the forest while H is similar during the morning and larger over pasture in the afternoon. The next section below explores this differences further.

[37] The question has been raised whether deforestation can impact the sink for reactive gases such as ozone. This question was addressed using the ozone data and associated fluxes obtained at the pasture site [for details, see Sigler et al. (submitted manuscript, 2000)]. Figure 11 shows a strong diurnal variation of ozone fluxes whose maximum values reached about 0.2 micrograms (O_3) m^{-2} s^{-1}. Compared to fluxes obtained at the Reserva Ducke forest in Central Amazon [*Fan et al.*, 1990] during the wet season and under similar atmospheric conditions, the ozone fluxes at the pasture site were on average 30% lower. These values were obtained despite the higher ozone levels at the pasture site and may be attributed to two key processes. First, forests are aerodynamically more rough and thus higher mechanically generated turbulence can be expected to transport ozone from the atmosphere to deposition substrate (i.e., leaves). Second, forests emit large amounts of biogenic hydrocarbons which under low nitrogen levels serve as effective sink for ozone. Thus, if the results reported by *Fan et al.* [1990] are characteristic of forested sites in the Amazon during the wet season, we can conclude that deforestation could contribute to a net decrease ($\sim$30%) in the effectiveness of tropospheric ozone sink within the deforested regions of the Amazon basin. Such reduced sink may contribute to enhanced ambient ozone levels.

## 4.6. Energy and Momentum Exchange Inside and Outside the Canopy

[38] Modeling biosphere-atmosphere interactions over a tropical forest is a non trivial task. The density of the vegetation as seen from above might lead to a suggested topography with a given displacement height. The canopy in Rebio Jaru, which is representative of a large forested region, has a mean height of 35 m and some of the higher

tree branches reach up to 45 m. Below the canopy, vegetation is sparse and a semi confined atmospheric layer is defined. The turbulent exchange process taking place between the layer below and above the canopy define the "surface" fluxes that will feed the boundary layer and lead to cloud formation. Due to this complexity not captured by many surface/vegetation parameterizations, several modeling studies [e.g., *Silva Dias et al.*, 2002] have had to adjust parameters of the surface layer, vegetation and soil, at the forest with barely acceptable results concerning the development of realistic surface fluxes and mixed layer over forest in the Amazon. Over pasture, on the other hand, parameters are easily adjusted. This points out to the need to measure the interchange of energy and momentum between below canopy and above canopy to be able to validate model results.

[39] Fast response instruments (3D sonic-anemometers, thermometers and hygrometers), with a sampling rate of 16 Hz (except during three days, when the sampling rate was 60 Hz), were installed on a 60 m tall micrometeorological tower (10°4.706'S; 61°56.027'W, at heights of 21 m, 45 m and 67 m). Also, slow response instruments, operated at a sampling rate of 0.1 Hz, provided vertical profiles of wind velocity, temperature, specific humidity, incoming solar radiation, net radiation and photosynthetically active radiation (PAR). Figure 12 shows the position of the instruments on the tower.

[40] The behavior of the radiation measured above and inside the Rebio-Jaru forest can be summarized [*Manzi et al.*, 2000; *Moura et al.*, 2000] as:

1. a minimum global solar radiation albedo of 13.1% $\pm$ 1.1% and a minimum global photosynthetically active
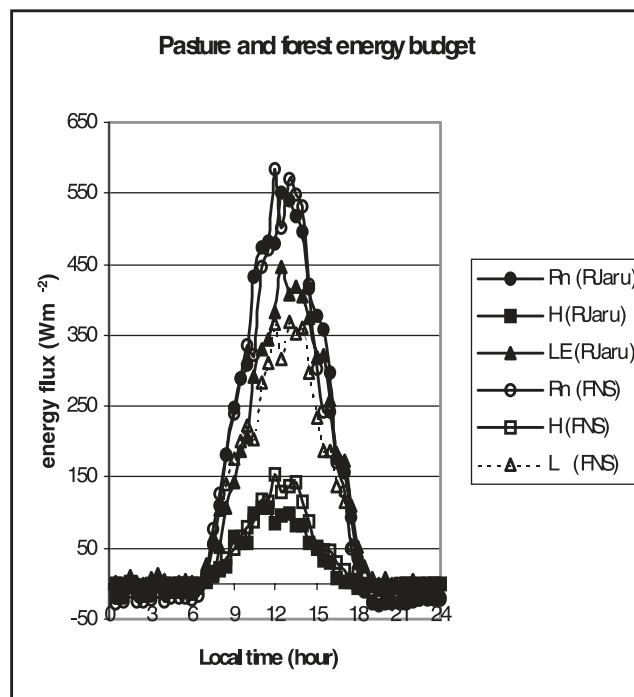
Figure 11. Average hourly ozone fluxes estimated for the pasture site in Rondônia during the wet season months of January and February 1999. The vertical bars denote standard deviations.
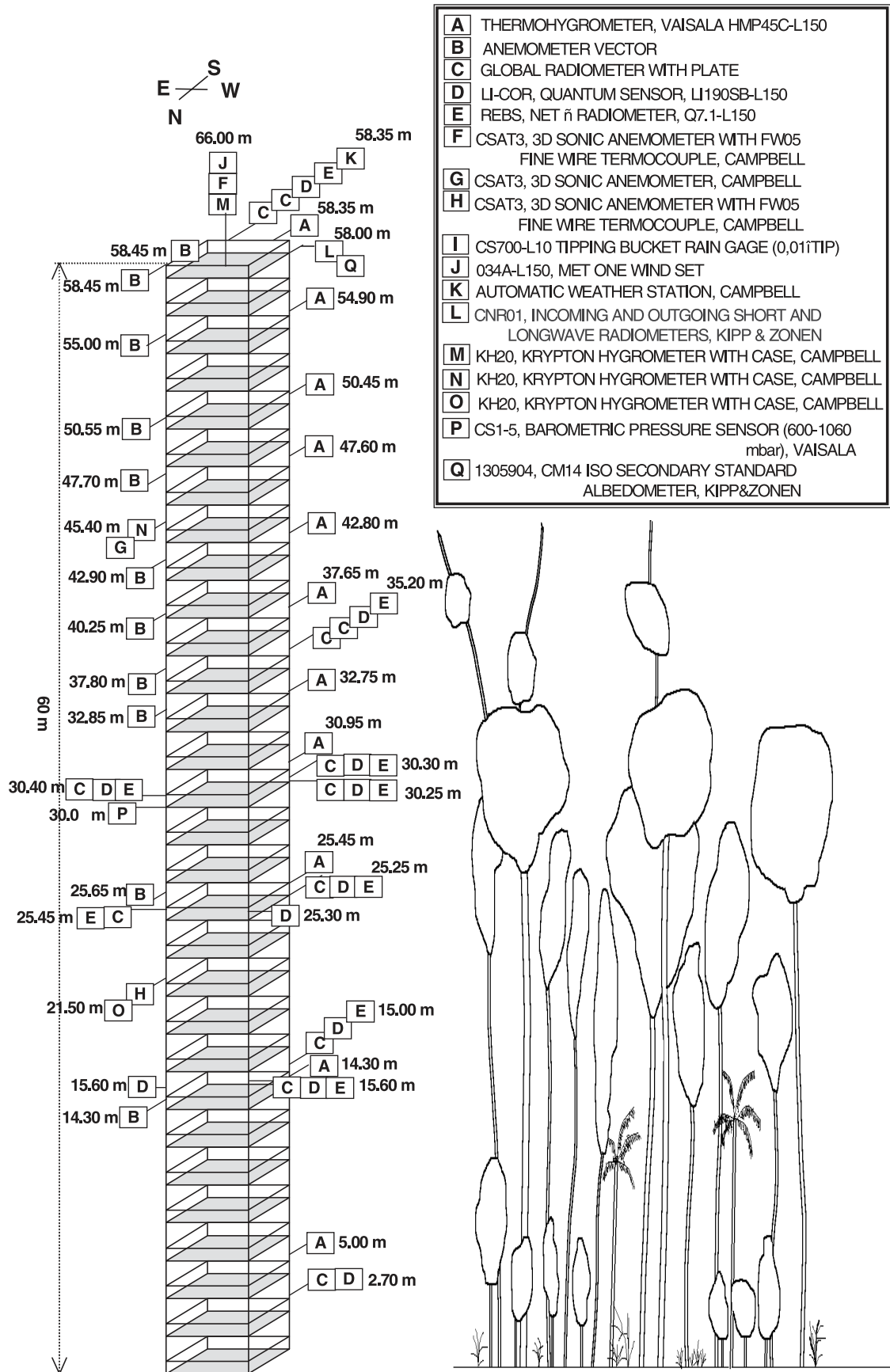
Figure 12. Schematic drawing of the micrometeorological tower located at Jaru Biological Reserve (Rebio-Jaru), with all instrumentation installed during the WETAMC/LBA.

radiation (PAR) albedo of 2.8% ± 0.3% was measured at the tower top near noon;

2. the penetration of radiation inside the canopy, determined by three five-level profiles (westward, southward and eastward of the tower) of net radiometers, PAR sensors and pyranometers, showed a rapid decrease in radiation intensity. Less than 40% of the PAR and incoming solar radiation above the forest reaches the 30 meter level (between 5 and 10 m below the canopy top) and only about 8% of the PAR and 14% of the solar radiation reaches the 15 meter level;

3. the radiation reaching the forest floor, measured by eight net radiometers, eleven PAR sensors and 12 pyranometers regularly distributed around the tower, at one meter above the ground, and integrated over five dry days between 0700 AM and 0500 PM (local time), was only 4.2% ± 2.0%, 1.6% ± 1.4% and 3.4% ± 2.2% of the radiation observed above the canopy, for net radiation, PAR and incoming solar radiation, respectively.

[41] A general result concerning the roughness characteristics of the forest is the determination of the zero-plane displacement. The methods used by *Molion and Moore* [1983] and by *De Bruin and Moore* [1985] were used, with the following results, respectively: $d = 26.6 ± 0.6$ m, $z_o = 3.6 ± 0.7$ and $d = 25.0 ± 2.3$ m, $z_o = 1.8 ± 0.6$ m. These results may be compared with the ones obtained by *Viswanadham et al.* [1990] at the reserve Reserva Ducke ($2°57'$S; $59°57'$W), Central Amazonia, $d = 30.9 ± 0.4$ m and $z_o = 2.2 ± 0.1$ m, obtained using Molion and Moore's method, and suggest that there are differences between these forests due to different heights and capacity to absorb momentum.

[42] One interesting aspect concerning the energy and momentum exchanges studied at Rebio Jaru is the difficulty to estimate the frequency associated with the spectral gap: the analysis of variance of the vertical component of the wind and of the temperature do not show a clear relative minimum, even when the sample segment was considerably increased (from 20 min to 3 hours). According to *von-Randow et al.* [2002], this difficulty may be attributed to the possible occurrence of factors such as the existence of local circulation and isolated eddies, which may introduce low frequency fluctuations to the turbulent signal. These factors probably occur in the flow studied here because: (1) the forest at Rebio Jaru is bordered at its western side by strips of deforested areas (the *fish-bone*), which may induce local circulation due to differences in the energy balance between the *fish-bone* surface and the forest; (2) the existence of thermal convection and consequent generation of cumulus clouds above the region creates a physical mechanism that provides the existence of intense alternating upward and downward motions (updrafts and downdrafts).

[43] The coupling characteristics of the flow above and below forest canopies have been studied by many authors both in experimental investigations [e.g., *Bosveld et al.*, 1999; *Brunet and Irvine*, 2000; *Fitzjarrald et al.*, 1990; *Jacobs et al.*, 1994; *Kruijt et al.*, 2000; *Mahrt et al.*, 2000; *Shuttleworth et al.*, 1985; *Shuttleworth*, 1989; *Raupach and Thom*, 1981] and in modeling [e.g., *Garratt*, 1992; *Shen and Leclerc*, 1997]. Many of these studies have indicated that turbulent exchange characteristics between the atmosphere and the canopy are not totally similar and depend on the specific morphological and physiological properties of
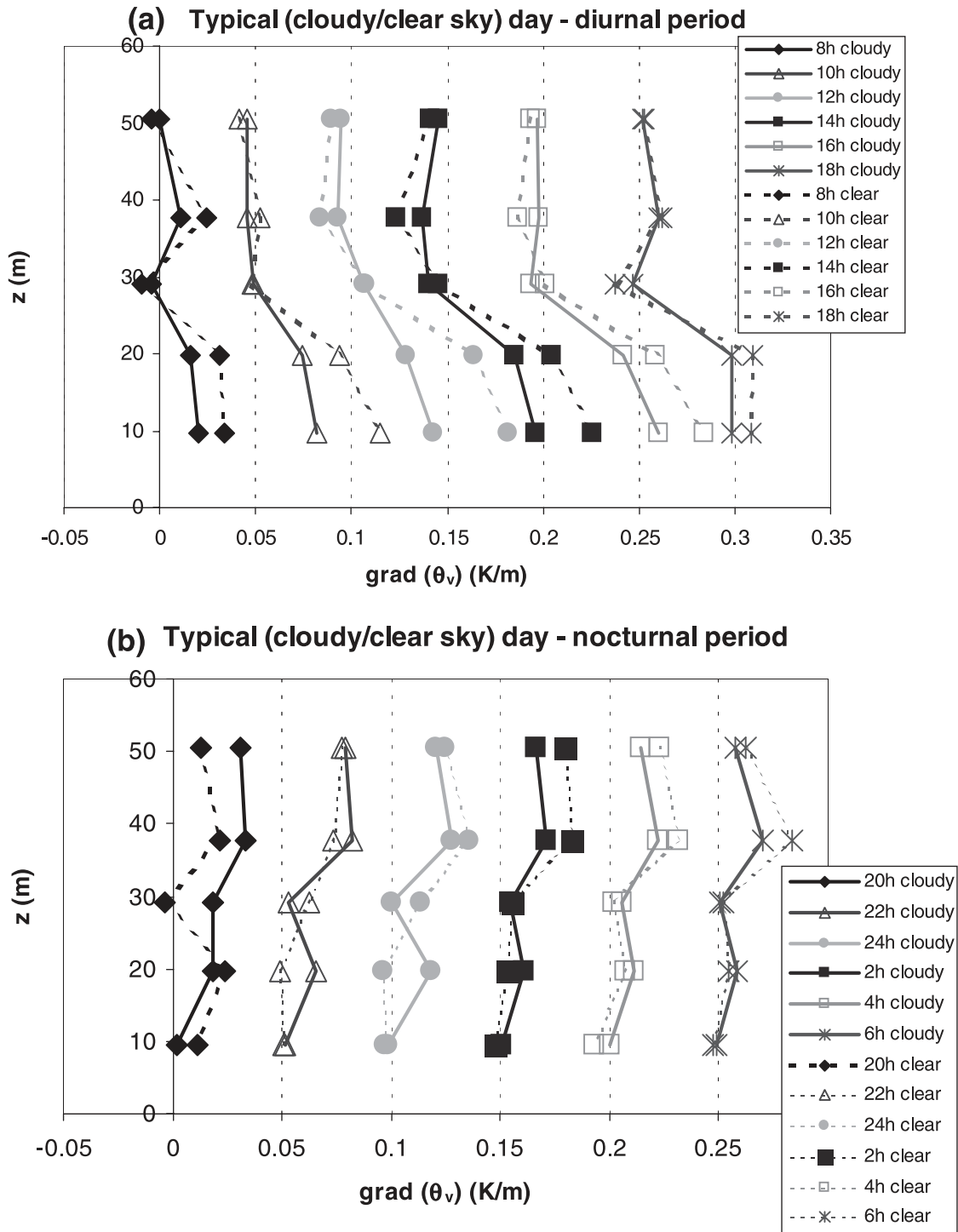
each particular forest site. For these reasons the mean wind velocity and virtual potential temperature profiles measured on the 60 m height micrometeorological tower have been analyzed.

[44] The 10 cup anemometers and 10 thermohygrometers were vertically placed according to Figure 12 with the objective to measure virtual potential temperature gradients above the canopy, below the canopy and the interface level between the canopy and the atmosphere. The results seem to confirm the suggestions of many authors [*Fitzjarrald et al.*, 1990; *Raupach et al.*, 1996; *Brunet and Irvine*, 2000] for whom the wind shear and the existence of an inflexion point in the wind velocity vertical profile are two physical factors which play an important role on the momentum exchange mechanism between the above and the inside canopy flows. The height interval which presents more data scattering is the one located next the canopy top, between 28 and 32 m above the ground. This scattering is stronger in sunny days and is less pronounced in cloudy situations. As shown by *Shen and Leclerc* [1997] in their study on large eddy simulation (LES) of kinetic turbulent energy budget above and inside forest canopy, the intensity of the convective activity above the vegetation influences the mean wind field in both regions, above and below canopy. More scattering at the top of the canopy in sunny days is due to the particular morphology of the forest structure with gaps that allow light to get into the canopy and wind to penetrate downwards. In this way, it is possible to have thermal gradients inside the canopy in sunny days, which may generate local circulations in this region and more intense mixing inside the canopy top region. In such situations, we expect to have lower virtual potential temperature vertical gradients compared to the gradients measured inside more closed forest canopies such as the one near Manaus, in the central part of the Amazon forest [*Shuttleworth et al.*, 1985]. Figure 13 shows the virtual potential temperature gradient measured inside and below the Amazon forest in Rondônia in a typical sunny day.

[45] The study of the characteristics of the turbulent fields above and below the canopy provides interesting information about: the nature of the interaction processes; the range of scales in which the turbulent exchange are intensive; the self-similar character of the turbulence for momentum and scalar fluctuations. This is useful in parameterizing the small-scale turbulent processes which is particularly useful in large-eddy simulations. *Bolzan et al.* [2002] have studied the probability density function (PDF) of velocity and temperature differences in the surface boundary layer of Amazonia based in the Tsallis' generalized thermostatistics theory. *Ramos et al.* [2001] have recently shown that this new approach provides a simple and accurate framework for modeling the statistical behavior of fully developed turbulence.

4.7. Local Effects of Deforestation on Boundary Layer Depth and Shallow Cumulus Clouds in the Wet Season

[46] The evolution of the convective boundary layer has a direct influence on the evolution of cloudiness and provides the link between the surface and the atmosphere. One of the striking features of convective boundary layer evolution in Rondônia in the wet season is that it is different from the dry season evolution at a deforested site as discussed by *Fisch et al.* [2000]. Basically, the large differences observed in the

(a)   Typical (cloudy/clear sky) day - diurnal period

(b)   Typical (cloudy/clear sky) day - nocturnal period

Figure 13. Vertical gradients of virtual potential temperature, with height, averaged during 3 cloudy (full lines) and 3 clear-sky (dashed lines) days. They are presented for every two hours, during diurnal (a) and nocturnal period (b). To provide a better visualization the values of each time step (pairs of cloudy/ clear sky curves) are incremented by 0.05 K m^{-1}.

dry season between forest and pasture mixed layer heights are due to the high values of surface sensible heat fluxes in the pasture with mixed layer height reaching 1600 m while the mixed layer reaches 1000 m in the forest. This pattern is substituted during the wet season by a situation where the boundary layer reaches about the same height over pasture and forest, as an average about 1000 m, with a tendency of the forest mixed layer heights to be about 100 m deeper. Referring back to Figure 10, the evolution early in the morning is a result of energy partition that favors a lower lifting condensation level (LCL) over forest and a faster growth. Figure 14 show the temperature and pressure difference from the surface to the LCL for 7 February 1999. The convective development throughout this day is
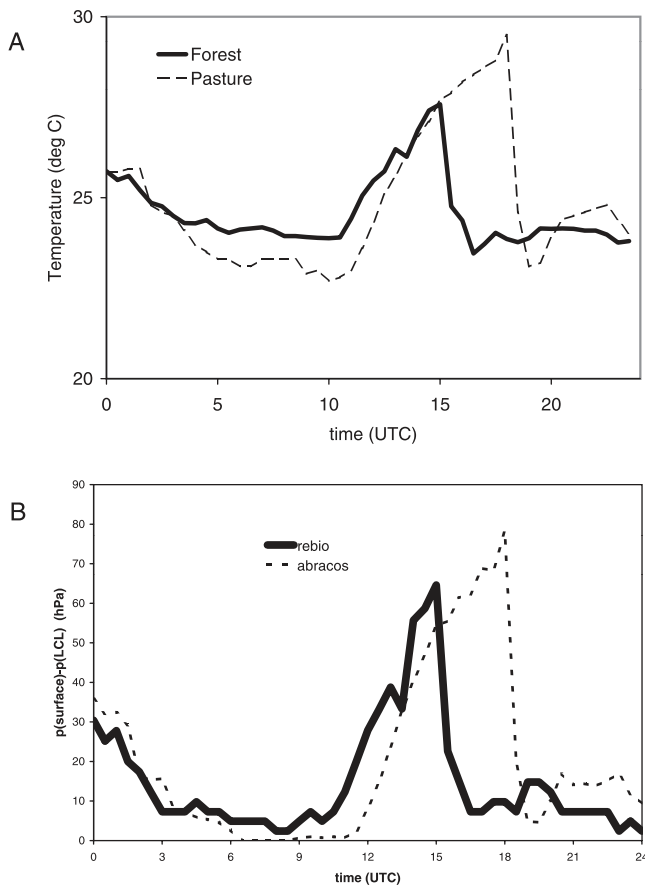
Figure 14. Surface data for 7 February 1999 at ABRACOS and REBIO JARU. (a) Temperature and (b) pressure difference between surface and lifting condensation level (LCL).

discussed further by *Silva Dias et al.* [2002]. Figure 14 shows an example of a day which starts sunny and clear, and the surface temperature evolution is associated with a faster evolution of the mixed layer over forest. After rains start at different times over forest and pasture, in this particular day, the continuous evolution is broken.

[47] The topography of Rondônia is such that deforestation occurs in valleys while mountain tops are forested. The effect of deforestation may be important for the shallow cumulus distribution but the effect of this on rainfall are still a subject of research. Cases like the one of 7 February 1999, modeled by *Silva Dias et al.* [2002], may be triggered by topography and enhanced by deforestation; however, more intense cases like the one in 26 January 1999 described by *Pereira Filho et al.* [2002], and by *Cifelli et al.* [2002] or the one in 17–18 February described by *Betts et al.* [2002a, 2002b] probably do not have a memory of the surface over which they were developed or may not be sensitive to the surface over which they propagate over their lifetime. *Laurent et al.* [2002], examining convection over the whole Amazon Basin have shown a tendency for mesoscale convective systems to initiate over high terrain.

[48] The location and average time of convection initiation have been identified by *Pereira et al.* [2000] using TOGA (C band, Doppler) and S-Pol (S band, Doppler, polarimetric) radars, for January and February (Wet Season)

and November (end of Dry Season) of 1999 during the WETAMC-LBA and TRMM-LBA (see locations in Figure 3. The results show that on average the convection starts only 30 min earlier in the wet season than in the end of the dry season. During the wet season, 70% of the days analyzed showed convection starting over areas with an altitude greater than 300 m. On the other hand, in the end of the dry season, only 45% of the days showed convection forming over areas with an altitude greater than 300 m. The days analyzed in January and February were also separated in to easterly or westerly prevailing flow, depending on the general motion of the cells during the day. In a westerly regime shallow cumulus start more randomly while during the easterly regime they show a preference for higher altitude and forest. *Rutledge et al.* [2001] using the S-Pol data indicate that forested regions of the S-POL domain were characterized by more rain than nonforested regions. Their results also suggest that topography or land elevation appear to play an equal or greater role than deforestation in rain production over the Amazon and that effects of deforestation on rain production are more substantial over elevated terrain. However, since the radar data set is relatively limited, basically 2 months, it is suggested that this research should be expanded to a longer time period using satellite data.

[49] The timing of convection initiation over a particular land cover represents the end result of a series of coupled physical processes including local response to large-scale dynamics, radiation and energy budgets at the surface and the associated sensible and latent heat fluxes, and their impact on boundary layer turbulence and local thermodynamic conditions. The timing of convection initiation also represents an important element for numerical model diurnal cycle validation, indicating whether or not the integrated effect of all the physical parameterizations, mainly surface, boundary layer turbulence, shallow and deep convection, and radiative transfer parameterizations, are consistent in producing a realistic result. In this sense, further research on this subject is necessary.

4.8. Influence of the Water Vapor on the Longwave Radiative Transfer

[50] The representation of the biosphere-atmosphere exchanges of energy and gases (including water vapor) requires accurate parameterizations for the radiative fluxes at the surface. As an example, in the revised Simple Biosphere Model, SiB2 [*Sellers et al.*, 1996], both the shortwave and the longwave downward irradiances incident at the top of the biosphere are required as boundary values. The daytime and nighttime evolution of the surface layer is highly dependent on the surface radiation budget and determine the stability of the surface layer which will ultimately affect the model ability to produce clouds.

[51] The relevancy of the water vapor in shortwave and longwave radiative transfer is well-known, and recent studies have reached a good agreement between spectral measurements and computations throughout the shortwave [*Mlawer et al.*, 2000] and the longwave wavelength domains [e.g., *Han et al.*, 1997]. Nevertheless, the representation of the water vapor absorption in general circulation models is a recurrent matter of discussion [*Ellingson*

Table 3. Computed and Measured Atmospheric Irradiances at the Fazenda Nossa Senhora Site During the Night of 19–20 February 1999[a]

Radiosonde Ascent	WVC (kg m^{-2})	E(LBL) (W m^{-2})	E(PIR) (W m^{-2})	E(CG1) (W m^{-2})
19 February 1999, 2343 UTC	48.3	386.4	374.2 (−3.2%)	381.8 (−1.2%)
20 February 1999, 0250 UTC	48.4	384.8	376.9 (−2.1%)	383.7 (−0.3%)
20 February 1999, 0607 UTC	48.2	385.7	372.4 (−3.5%)	380.3 (−1.4%)
20 February 1999, 0846 UTC	48.0	379.1	371.7 (−2.0%)	378.0 (−0.3%)

[a] WVC is the column-integrated water vapor content, E(LBL) is the irradiance computed through the line-by-line radiative transfer code, E(PIR) is the irradiance measured with an Eppley PIR pyrgeometer, and E(CG-1) is the irradiance measured with a Kipp & Zonen CG-1 pyrgeometer. Numbers between parentheses indicate relative deviations from E(LBL) results.

et al., 1991]. The extreme conditions of moisture (larger than 45 kg m^2 of column-integrated water vapor content) in the Amazon region pose a challenge on the reliability of radiation parameterizations.

[52] Addressing the field validation of longwave radiation calculations was the objective of detailed measurements performed during WETAMC and TRMM/LBA. Basically, measurements of the downward longwave irradiance near the ground (hereafter, atmospheric irradiance) were performed at the pasture site with two different pyrgeometers. As a first attempt of field validation and due to the absence of cloudless periods longer than a few minutes during the field campaign, the main efforts have been dedicated to the role played by the water vapor present in the lower troposphere on the longwave radiative transfer.

[53] Table 3 compares computed and measured atmospheric irradiances for the available coincidences of soundings and pyrgeometer data at pasture site during the night of 19–20 February 1999. According to a careful analysis of the GOES-8 satellite imagery over the region, this night was associated with a transient cover of middle and high clouds. The nearby automated weather station indicated a slow cooling of the first 10 meters above ground and relative humidity values close to 100% throughout this layer.

[54] Irradiances E(LBL) in this table were obtained through an updated version of the line-by-line radiative transfer model developed by *Fomin* [1995], by taking into account the effects of thousands of absorption lines due to water vapor, carbon dioxide, and ozone over the wave number domain 0–3000 cm^{-1}. Very similar E(LBL) values, 0.5% or 2 W m^{-2} smaller, were obtained by neglecting the atmospheric layers above 6 km of altitude. A detailed analysis of irradiance values integrated over 100 cm^{-1} spectral bands indicated that such "longwave" top of the atmosphere could be placed still closer to the ground throughout large spectral domains, affected by strong water vapor and carbon dioxide absorption lines. In the case of the "window" 1000–1100 cm^{-1} band, the neglect of 0.5% would correspond to a top of the atmosphere at 30 km. In other words, the night of 19–20 February 1999 was characterized by a so high water vapor content that the middle and high regions of the troposphere would be inefficient to provide radiant energy near the ground. Therefore, the occurrence of middle and high clouds above very high water vapor contents would be poorly detected by pyrgeometers, which furnish irradiances integrated over the wave number domain of 0–3000 cm^{-1}.

[55] Table 3 indicates a systematic bias (about 2%) between measured irradiances E(PIR) and E(CG1) provided by different commercial pyrgeometers. Such a bias could be associated with their design (influence of thermal gradients,

etc) as well as with calibration issues. Measured irradiances were consistently smaller during the night of 19–20 February 1999 than the respective computations performed by assuming absence of clouds. The proper representation of middle and high clouds would increase the irradiances E(LBL), because their emitting strength is greater than the molecular absorbers taken into account. The inclusion of other molecular absorbers would increase E(LBL) by 1.5 W m^{-2} [*Clough and Iacono*, 1995]. The disagreement between computations and measurements remains unexplained, and it is possible that it will be understood only under true cloudless conditions. Additional efforts are being devoted in improving the line-by-line radiative transfer model employed in the present (water vapor continuum approach, vertical integration scheme, etc). The absolute accuracy of measured irradiances E(PIR) and E(CG1) remains also a subject of discussion.

5. Conclusions and Scientific Challenges

[56] The main results of the WETAMC/LBA and TRMM/LBA field campaign are the following:

1. the wet season in the Amazon region is affected by intraseasonal oscillations that are seen locally as different large-scale forcing; the SACZ produces locally low level convergence and zonal winds with a westerly component; during breaks of the SACZ, there is no significant low level large-scale forcing and winds are from the east.

2. The westerly and easterly wind regimes are associated with different modes of convection, deep isolated convection during easterlies and more stratiform, widespread and shallow convection during westerlies; CCN concentrations are higher during the easterly regime that during the westerly regime.

3. Deforestation seems to be of secondary importance during the wet season as compared to the dry season. However, there are differences between forest and pasture in the radiation budget and in the surface fluxes. There is a complex interaction between cloudiness and surface fluxes during the wet season leading to different times of initiation of first clouds. Mixed layer heights grow faster over forest and reach about the same maximum values in the afternoon as over pasture in the wet season. Shallow clouds form first over forest and, on the average, 30 min later over pasture. Deforestation may represent a reduced sink for ozone as compared to forest.

4. There are indications that mesoscale convective systems are initiated over high terrain. Deforestation may be enhancing rainfall.

5. The interaction between forest and atmosphere in the interface represented by the canopy affects mainly the

momentum fluxes. In a companion paper, *Andreae et al.* [2002] discusses the interactions affecting trace gases, which will eventually influence the biogenic portion of CCN.

6. Convective storms may have an impact of ozone budgets through convective downdrafts. The feedback on vegetation and back to the atmosphere are yet unknown.

7. The very moist atmosphere in Rondônia in the wet season constitutes a challenge not only for longwave radiation parameterizations employed in numerical models, but also for relatively detailed line-by-line radiative transfer codes. Anyway, the longwave radiative transfer near the ground seems independent on the occurrence of middle and high clouds; thus, simplified formulations for estimating atmospheric irradiance near the ground (which are strictly valid under clear sky conditions) may be successful over a broad range of atmospheric conditions.

[57] The LBA-TRMM joint effort has surely produced the most comprehensive database ever gathered from a tropical continent in atmospheric and related sciences, a land-based GATE (GARP-Global Atmospheric Research Program-Atlantic Tropical Experiment), or TOGA-COARE (Tropical Ocean Global Atmosphere-Coupled Ocean Atmosphere Response Experiment), but more interdisciplinary. The preliminary results outlined above are just scratching the surface and surely have raised more questions than answers.

[58] One of the main scientific challenges that are posed from the results outlined above is, of course, the modeling of the complete atmosphere biosphere interaction including the role of vegetation, the atmospheric chemistry processes, the full interaction with radiation of trace gases, aerosol and clouds, and the atmospheric dynamics and thermodynamics evolution. The complete answer to the basic LBA questions on

1. How does Amazonia currently function as a regional entity?

2. How will changes in land use and climate affect the biological, chemical and physical functions of Amazonia, including the sustainability of development in the region and the influence of Amazonia on global climate?

is based on the ability to model and simulate all the processes involved in a coupled way. While this is still a far-reaching goal, the analysis of the WETAMC/LBA and TRMM/LBA data and the new questions posed are a step in the direction of the understanding of the Amazon environment.

[59] The relationship between clouds and the surface, from the point of view of surface fluxes, was expected. The role of CCN with a biogenic origin poses a new dimension to the understanding of cloud evolution and its relation to deforestation in the Amazon and raises questions that will have to be addressed possibly through modeling. Focus on the transition season, between the dry and wet season, may bring new lights to the question of the relative role of CCN in different large-scale scenarios.

[60] The coupling of the several disciplines involved in understanding moist convection in the Amazon is certainly one of the major challenges faced in the upcoming years of LBA.

References

Alvalá, R. C. S., et al., Intra diurnal and seasonal variability of soil temperature, heat flux, soil moisture content and thermal properties under forest and pasture in Rondônia, *J. Geophys. Res.*, *107*, 10.1029/2000JD000337, in press, 2002.

Anagnostou, E. N., and C. A. Morales, Rainfall estimation from TOGA radar observations during LBA field campaign, *J. Geophys. Res.*, *107*, 10.1029/2000JD000337, in press, 2002.

Andreae, M. O., et al., Biogeochemical cycling of carbon, water, energy, trace gases and aerosols in Amazonia: The LBA-EUSTACH experiments, *J. Geophys. Res.*, *107*, 10.1029/2001JD000324, in press, 2002.

Artaxo, P., J. V. Vanderlei Martins, M. A. Yamasoe, A. S. Procópio, T. M. Pauliquevis, M. O. Andreae, P. Guyon, L. V. Gatti, and A. M. Cordova Leal, Physical and chemical properties of aerosols in the wet and dry seasons in Rondônia, Amazônia, *J. Geophys. Res.*, *107*, 10.1029/2001JD000666, in press, 2002.

Bell, G. D., M. S. Halpert, C. F. Ropelewski, V. E. Kousky, A. V. Douglas, R. C. Schnell, and M. E. Gelman, Climate assessment for 1998, *Bull. Am. Meteorol. Soc.*, *80*(5), S1–S48, 1999.

Betts, A. K., and C. Jacob, Evaluation of the diurnal cycle of precipitation, surface thermodynamics and surface fluxes in the ECMWF model using LBA data, *J. Geophys. Res.*, *107*, 10.1029/2001JD000427, in press, 2002.

Betts, A. K., J. D. Fuentes, M. Garstang, and J. H. Ball, Surface diurnal cycle and boundary layer structure over Rondônia during the rainy season, *J. Geophys. Res.*, *107*, 10.1029/2000JD000158, in press, 2002a.

Betts, A. K., L. Gatti, M. A. F. Silva Dias, and J. Fuentes, Transport of ozone to the surface by downdrafts at night, *J. Geophys. Res.*, *107*, 10.1029/2000JD000158, in press, 2002b.

Bolzan, M. J. A., F. M. Ramos, L. D. A. Sá, C. R. Neto, and R. R. Rosa, Analysis of fully developed turbulence above and below Amazon forest canopy using Tsallis' generalized thermostatistics, *J. Geophys. Res.*, in press, 2002.

Bosveld, F. C., A. A. M. Holtslag, and B. J. J. M. Van Den Hurk, Nighttime convection in the interior of a dense Douglas fir forest, *Boundary Layer Meteorol.*, *93*, 171–195, 1999.

Braud, I., A. C. Dantas-Antonino, M. Vauclin, J. L. Thony, and P. Ruelle, A simple soil plant atmosphere transfer model (SiSPAT): Development and field verification, *J. Hydrol.*, *166*, 213–250, 1995.

Brunet, Y., and M. R. Irvine, The control of coherent eddies in vegetation canopies: Streamwise structure spacing, canopy shear scale and atmospheric stability, *Boundary Layer Meteorol.*, *94*, 139–163, 2000.

Carey, L. D., R. Cifelli, W. A. Petersen, S. A. Rutledge, and M. A. F. Silva Dias, Characteristics of Amazonian rain measured during TRMM-LBA, paper presented at *30th Conference on Radar Meteorology*, p. 12A.9, Am. Meteorol. Soc., Boston, Mass., 2001.

Carvalho, L. M. V., C. Jones, and M. A. F. Silva Dias, Intraseasonal large-scale circulations and mesoscale convective activity in tropical South America during the TRMM-LBA campaign, *J. Geophys. Res.*, *107*, 10.1029/2001JD000745, in press, 2002.

Cifelli, R., W. A. Petersen, L. D. Carey, S. A. Rutledge, and M. A. F. Silva Dias, Radar observations of kinematic, microphysical, and precipitation characteristics of two MCSs in TRMM-LBA, *J. Geophys. Res.*, *107*, 10.1029/2000JD000264, in press, 2002.

Clough, S. A., and M. J. Iacono, Line-by-line calculation of atmospheric fluxes and cooling rates, 2, Application to carbon dioxide, ozone, methane, nitrous oxide and the halocarbons, *J. Geophys. Res.*, *100*, 16,519–16,535, 1995.

Cohen, J. C., M. A. F. Silva Dias, and C. Nobre, Climatological aspects of Amazon squall lines (in Portuguese Aspectos climatológicos das linhas de instabilidade na Amazônia), *Climanálise*, *4*(11), 34–40, 1989.

Cohen, J. C. P., M. A. Silva Dias, and C. A. Nobre, Environmental conditions associated with Amazonian squall lines: Case study, *Mon. Weather Rev.*, *123*, 3163–3174, 1995.

Cutrim, E., D. W. Martin, and R. Rabin, Enhancement of cumulus clouds over deforested lands in Amazonia, *Bull. Am. Meteorol. Soc.*, *76*(10), 1801–1805, 1995.

De Bruin, H. A. R., and C. J. Moore, Zero-plane displacement and rough-

ness length for tall vegetation, derived from a simple mass conservation hypothesis, *Boundary Layer Meteorol.*, *31*, 39–49, 1985.

DeMaria, M., Linear response of a stratified tropical atmosphere to convective forcing, *J. Atmos. Sci.*, *42*, 1944–1959, 1985.

Douglas, M. W., and M. Peña, The Pan American Climate Studies Sounding Network (PACS-SONET) recent history and planned improvements, paper presented as Extended Abstracts at the *6th International Conference on Southern Hemisphere Meteorology and Oceanography, 3–7 April 2000, Santiago, Chile*, pp. 258–259, Am. Meteorol. Soc., Boston, Mass., 2000.

Ellingson, R. G., J. Ellis, and S. Fels, The intercomparison of radiation codes used in climate models: Long wave results, *J. Geophys. Res.*, *96*, 8929–8953, 1991.

Fan, S. M., S. C. Wofsy, P. S. Bakwin, D. J. Jacob, and D. R. Fitzjarrald, Atmosphere-biosphere exchange of CO_2-O_3 in the central Amazon forest, *J. Geophys. Res.*, *95*, 16,851–16,864, 1990.

Fisch, G., A. D. Culf, and C. A. Nobre, Modelling convective boundary layer growth in Rondonia, in *Amazonian Deforestation and Climate*, edited by J. H. C. Gash et al., pp. 425–436, John Wiley, New York, 1996.

Fisch, G., J. Tota, L. Machado, B. Ferrier, M. Silva Dias, A. J. Dolman, J. Halverson, and J. Fuentes, Atmospheric boundary layer growth during the LBA/TRMM experiment, Proceedings 15th Conference on Hydrology, paper presented at the *80th AMS Annual Meeting, Long Beach, Calif., 9–14 January*, pp. 319–322, Am. Meteorol. Soc., Boston, Mass., 2000.

Fitzjarrald, D. R., K. E. Moore, O. M. R. Cabral, J. Scolar, A. O. Manzi, and L. D. A. Sá, Daytime turbulent exchange between the Amazon forest and the atmosphere, *J. Geophys. Res.*, *95*, 16,825–16,838, 1990.

Fomin, B. A., Effective interpolation technique for line-by-line calculations of radiation absorption in gases, *J. Quant. Spectrosc. Radiat. Transfer*, *53*(6), 663–669, 1995.

Formenti, P., M. O. Andreae, L. Lange, G. Roberts, J. Cafmeyer, I. Rajta, W. Maenhaut, B. N. Holben, P. Artaxo, and J. Lelieveld, Saharan dust in Brazil and Suriname during the Large-Scale Biosphere-Atmosphere Experiment in Amazonia (LBA)-Cooperative LBA Regional Experiment (CLAIRE) in March 1998, *J. Geophys. Res.*, *106*, 14,919–14,934, 2001.

Gandu, A. W., and P. L. Silva Dias, Impact of tropical heat sources on the South American tropospheric upper circulation and subsidence, *J. Geophys. Res.*, *103*, 6001–6015, 1998.

Garratt, J. R., *The Atmospheric Boundary Layer*, 316 pp., Cambridge Univ. Press, New York, 1992.

Garstang, M., et al., Amazon coastal squall lines, part 1, Structure and kinematics, *Mon. Weather Rev.*, *122*, 608–622, 1994.

Gash, J. H. C., A. Nobre, J. M. Roberts, and R. L. Victoria, An overview of ABRACOS, in *Amazon Deforestation and Climate*, edited by Gash et al., pp. 1–14, John Wiley, New York, 1996.

Greco, S., R. Swap, M. Garstang, S. Ulanski, M. Shipham, R. C. Harris, R. Talbot, M. O. Andreae, and P. Artaxo, Rainfall and surface kinematics conditions over central Amazonia during ABLE 2B, *J. Geophys. Res.*, *95*, 17,001–17,014, 1990.

Greco, S., J. Scala, J. Halverson, H. L. Massie, W. K. Tao, and M. Garstang, Amazon coastal squall lines, 2, Heat and moisture transports, *Mon. Weather Rev.*, *122*, 623–635, 1994.

Gregory, G. L., E. V. Browell, and L. S. Warren, Boundary layer ozone: An airborne survey above the Amazon basin, *J. Geophys. Res.*, *93*, 452–1468, 1988.

Grimm, A. M., and P. L. Silva Dias, Analysis of tropical extratropical interactions with influence functions of a barotropic model, *J. Atmos. Sci.*, *52*, 3538–3555, 1995.

Han, Y., J. A. Shaw, J. H. Churnside, P. D. Brown, and S. A. Clough, Infrared spectral radiance measurements in the tropical Pacific atmosphere, *J. Geophys. Res.*, *102*, 4353–4356, 1997.

Harris, R. C., et al., The Amazon Boundary Layer Experiment (ABLE-2A): Dry season 1985, *J. Geophys. Res.*, *93*, 1351–1360, 1988.

Harris, R. C., et al., The Amazon Boundary Layer Experiment (ABLE-2B): Wet season 1987, *J. Geophys. Res.*, *95*, 16,721–16,736, 1990.

Herdies, D. L., A. da Silva, and M. A. F. Silva Dias, The bi-modal pattern of the summer circulation over South America, *J. Geophys. Res.*, *107*, 10.1029/2001JD000997, in press, 2002.

Horel, J., A. Hahmann, and J. Geiler, An investigation of the annual cycle of the convective activity over the tropical Americas, *J. Clim.*, *2*, 1388–1403, 1989.

Jacobs, A. F. G., J. H. Van Boxel, and R. M. M. El-Kilani, Nighttime free convection characteristics within a plant canopy, *Boundary Layer Meteorol.*, *71*, 375–391, 1994.

Kayano, M. T., and V. E. Kousky, Zonally symmetric and asymmetric features of the tropospheric Madden–Julian oscillation, *J. Geophys. Res.*, *103*, 13,703–13,712, 1998.

Kirchhoff, V. W. J. H., I. M. O. Da Silva, and E. V. Browell, Ozone measurements in Amazonia: Dry season versus wet season, *J. Geophys. Res.*, *95*, 16,913–16,926, 1990.

Kirkman, G. A., A. Gut, C. Ammann, L. V. Gatti, M. A. L. Moura, and F. X. Meixner, Surface exchange of nitric oxide, nitrogen dioxide and ozone at a cattle pasture in Rondonia, Brazil, *J. Geophys. Res.*, *107*, 10.1029/2001JD000523, in press, 2002.

Kousky, V. E., and M. T. Kayano, Principal modes of outgoing longwave radiation and 250 mb circulation for the South-American sector, *J. Clim.*, *7*, 1131–1143, 1994.

Kruijt, B., Y. Malhi, J. Lloyd, A. D. Nobre, A. C. Miranda, M. G. P. Pereira, A. Culf, and J. Grace, Turbulence statistics above and within two Amazon rain forest canopies, *Boundary Layer Meteorol.*, *94*, 297–331, 2000.

Laurent, H., L. A. T. Machado, C. A. Morales, and L. Durieux, Characteristics of the Amazonian mesoscale convective systems observed from satellite and radar during the WETAMC/LBA experiment, *J. Geophys. Res.*, *107*, 10.1029/2001JD000337, in press, 2002.

LBA, *Concise Experimental Plan*, INPE, São José dos Campos, Brazil, 1996. Also available at http://lba.cptec.inpe.br.

Machado, L. A. T., H. Laurent, and A. A. Lima, The diurnal march of the convection observed during TRMM-WETAMC/LBA, *J. Geophys. Res.*, *107*, 10.1029/2001JD000338, in press, 2002.

Madden, R. A., and P. R. Julian, Observations of the 40–50-day tropical oscillation: A review, *Mon. Weather Rev.*, *122*, 814–837, 1994.

Mahrt, L., X. Lee, A. Black, H. Neumann, and R. M. Staebler, Nocturnal mixing in a forest subcanopy, *Agric. For. Meteorol.*, *101*, 67–78, 2000.

Maia Alves, S. F., G. Fisch, and I. F. Vendrame, Modificações do microclima e regime hidrológico devido ao desmatamento na Amazônia, *Acta Amazon.*, *29*(3), 395–409, 1999.

Manzi, A. O., et al., Measurements of PAR, solar and terrestrial radiation above forest and pasture sites in Rondônia, paper presented at *1st LBA Scientific Conference, Book of Abstracts, Belém, 26–30 June*, pp. 272–273, Minist. of Sci. and Technol., Brasilia, Brazil, 2000.

Marengo, J. A., M. Douglas, and P. Silva Dias, The South American low-level jet east of the Andes during the LBA-TRMM and WET AMC campaign of January–February 1999, *J. Geophys. Res.*, *107*, 10.1029/2001JD001188, in press, 2002.

Marton, E. and P. L. Silva Dias, Variabilidade intrasazonal na zona de Convergência do Atlântico Sul. (Intraseasonal variability of the South Atlantic Convergence Zone), paper presented at *IX Congreso Latinoamericano e Iberico de Meteorologia, 7–11 May, Buenos Aires, Argentina*, p. 179, Cent. Argen. de Meteor., Buenos Aires, Argentina, 2001.

Mlawer, E. J., P. D. Brown, S. A. Clough, L. C. Harrison, J. J. Michalsky, P. W. Kiedron, and T. Shippert, Comparison of spectral direct and diffuse solar irradiance measurements and calculations for cloud-free conditions, *Geophys. Res. Lett.*, *27*, 2653–2656, 2000.

Mohr, K. I., and E. J. Zipser, Mesoscale convective systems defined by their 85 GHz ice scattering signature: Size and intensity comparison over tropical oceans and continents, *Mon. Weather Rev.*, *124*, 2417–2437, 1996.

Mohr, K. I., J. S. Famiglietti, and E. J. Zipser, The contribution to tropical rainfall with respect to convective system type, size, and intensity estimated from the ice scattering signature, *J. Appl. Meteorol.*, *38*, 596–606, 1999.

Molion, L. C. B., and C. J. Moore, Estimating the zero-plane displacement for tall vegetation using a mass conservative method, *Boundary Layer Meteorol.*, *26*, 115–125, 1983.

Moura, R. G., J. Tota, A. O. Manzi, and L. Gu, Medidas e modelagem da radiação solar interceptada pela vegetação durante a estação chuvosa na floresta da REBIO-JARU, paper presented at *1st LBA Scientific Conference, Book of Abstracts, Belém, 26–30 June*, pp. 277–278, Minist. of Sci. and Technol., Brasilia, Brazil, 2000.

Negri, A. J., L. Xu, and R. F. Adler, A TRMM-calibrated infrared rainfall algorithm applied over Brazil, *J. Geophys. Res.*, *107*, 10.1029/2001JD000265, in press, 2002.

Nobre, C. A., P. J. Sellers, and J. Shukla, Amazonian deforestation and regional climate change, *J. Clim.*, *4*, 957–987, 1991.

Nogues-Paegle, J., and K. M. Mo, Alternating wet and dry conditions over South America during summer, *Mon. Weather Rev.*, *125*, 279–291, 1997.

Pereira, L. G. P., M. A. F. Silva Dias, A. J. Peeira Filho, and P. T. Matsuo, Timing of convection initiation during the WETAMC-LBA, paper presented at *1st LBA Scientific Conference, Book of Abstracts, 26–30 June*, p. 232, Minist. of Sci. and Technol., Brasilia, Brazil, 2000.

Pereira Filho, A., M. A. F. Silva Dias, R. I. Albrecht, L. G. P. Pereira, A. W. Gandú, and O. Massambani, Multi-sensor analysis of a squall line in the Amazon region, *J. Geophys. Res.*, *107*, 10.1029/2000JD000520, in press, 2002.

Petersen, W. A., and S. A. Rutledge, Regional variability in tropical convection: Observations from TRMM, *J. Clim.*, *14*, 3566–3586, 2001.

Petersen, W. A., S. A. Rutledge, R. Cifelli, and R. Blakeslee, Convective regimes observed during TRMM/LBA: An integrated view from TRMM satellite and Brazilian lightning detection network, *TRMM Workshop*, 2000.

Ramos, F. M., R. R. Rosa, C. Rodrigues Neto, M. J. A. Bolzan, L. D. A. Sá, and H. F. C. Velho, Nonextensive statistics and three-dimensional fully developed turbulence, *Physica A*, *295*, 250–253, 2001.

Rao, V. B., and K. Hada, Characteristics of rainfall over Brazil: Annual variations and connections with the southern oscillation, *Theor. Appl. Climatol.*, *42*, 81–91, 1990.

Raupach, M. R., and A. S. Thom, Turbulence in and above plant canopies, *Annu. Rev. Fluid Mech.*, *13*, 97–129, 1981.

Raupach, M. R., J. J. Finnigan, and Y. Brunet, Coherent eddies and turbulence in vegetation canopies: The mixing-layer analogy, *Boundary Layer Meteorol.*, *78*, 351–382, March, 1996.

Rickenbach, T. M., R. Nieto Ferreira, J. Halverson, D. L. Herdies, and M. A. F. Silva Dias, Modulation of convection in the south western Amazon basin by stationary fronts, *J. Geophys. Res.*, *107*, 10.1029/2001JD000263, in press, 2002.

Roberts, G. C., M. O. Andreae, J. Zhou, and P. Artaxo, Cloud condensation nuclei in the Amazon Basin: "Marine" conditions over a continent?, *Geophys. Res. Lett.*, *28*, 2807–2810, 2001.

Rosenfeld, D., TRMM observed first evidence of smoke from forest fires inhibiting rainfall, *Geophys. Res. Lett.*, *26*, 3105–3108, 1999.

Rutledge, S. A., W. A. Petersen, L. D. Carey, R. Cifelli, and M. A. F. Silva Dias, Synoptic, mesoscale and microphysical characteristics of convective systems observed during TRMM-LBA, paper presented at *4th International Scientific Conference on the Global Energy and Water Cycle, Book of Abstracts, 10–14 September*, p.14, World Meteor. Org., Geneva, Switzerland, 2001.

Sellers, P. J., D. A. Randall, G. J. Collatz, J. A. Berry, C. B. Field, D. A. Dazlich, C. Zhang, G. D. Collelo, and L. Bounoua, A revised land surface parameterization (SiB2) for atmospheric GCMs, part I, model formulation, *J. Clim.*, *9*, 676–705, 1996.

Shen, S., and M. Y. Leclerc, Modelling the turbulence structure in the canopy layer, *Agric. For. Meteorol.*, *87*, 3–25, November, 1997.

Shuttleworth, W. J., Micrometeorology of temperate and tropical forest, *Philos. Trans. R. Soc. London, Ser. B*, *324*(1223), 299–334, 1989.

Shuttleworth, J. W., et al., Daily variations of temperature and humidity within and above Amazonian forest, *Weather*, *40*(4), 102–108, 1985.

Silva Dias, M. A. F., Storms in Brazil, in *Hazards and Disasters Series, Storms Volume II*, edited by R. Pielke Sr. and R. Pielke Jr., pp. 207–219, Routledge, New York, 1999.

Silva Dias, M. A. F., and R. N. Ferreira, Application of a linear spectral model to the study of Amazonian squall lines, *J. Geophys. Res.*, *97*, 20,405–20,419, 1992.

Silva Dias, M. A. F., and P. Regnier, Simulation of mesoscale circulations in a deforested area of Rondonia in the dry season, in *Amazonian Deforestation and Climate*, edited by J. Gash et al., pp. 531–547, John Wiley, New York, 1996.

Silva Dias, P. L., W. H. Schubert, and M. DeMaria, Large-scale response of the tropical atmosphere to transient convection, *J. Atmos. Sci.*, *40*, 2689–2707, 1983.

Silva Dias, P. L., M. A. F. Silva Dias, and D. S. Moreira, Mesoscale reanalysis, Proceedings 15th Conference on Hydrology, paper presented at *80th AMS Annual Meeting, Long Beach, Calif., 9–14 January*, Am. Meteorol. Soc., Boston, Mass., 2000.

Silva Dias, M. A. F., et al., A case study of the organization of convection into precipitating convective lines in the southwest Amazon, *J. Geophys. Res.*, *107*, 10.1029/2001JD000375, in press, 2002.

Souza, E. P., N. O. Rennó, and M. A. F. Silva Dias, Convective circulations induced by surface heterogeneities, *J. Atmos. Sci.*, *57*, 2915–2922, 2000.

Tokai, A., A. Krueger, W. F. Krajewski, and A. J. Pereira Filho, Measurements of drop size distribution in southwestern Amazon Basin, *J. Geophys. Res.*, *107*, 10.1029/2001JD000358, in press, 2002.

Tota, J., G. Fisch, P. J. Oliveira, J. D. Fuentes, and J. Siegler, Variabilidade da precipitação em área de pastagem durante o experimento LBA/TRMM, *Acta Amazon.*, *30*(4), 305–318, 2000.

Van Wijk, W. R., *Physics of Plant Environment*, 382 pp., North-Holland, New York, 1963.

Viswanadham, Y., L. C. B. Molion, A. O. Manzi, L. D. A. Sá, V. P. Silva Filho, R. G. B. André, J. L. M. Nogueira, and R. C. Dos Santos, Micrometeorological measurements in Amazon forest during GTE/ABLE-2A mission, *J. Geophys. Res.*, *95*, 13,669–13,682, 1990.

Von Randow, C., L. D. A. Sá, G. S. S. D. Prasad, A. Manzi, P. R. A. Arlino, and B. Kruijt, Scale variability of atmospheric surface layer fluxes of energy and carbon over a tropical rain forest in south-west Amazonia, I, Diurnal conditions, *J. Geophys. Res.*, in press, 2002.

Wang, J., R. Bras, and E. A. B. Eltahir, The impact of observed deforestation on the mesoscale distribution of rainfall and clouds in Amazonia, *J. Hydrometeorol.*, *1*(6), 267–286, 2000.

Williams, E., et al., Contrasting convective regimes over the Amazon: Implications for cloud electrification, *J. Geophys. Res.*, *107*, 10.1029/2001JD000380, in press, 2002.

Wright, I. R., J. H. C. Gash, H. R. Da Rocha, W. J. Shuttleworth, C. A. Nobre, G. T. Maitelli, C. A. G. P. Zamparoni, and P. R. A. Carvalho, Dry season micrometeorology of central Amazonian ranchland, *Q. J. R. Meteorol. Soc.*, *118*(508), 1083–1099, 1992.

Zipser, E. J., The role of organized unsaturated convective downdrafts in the structure and rapid decay of an equatorial disturbance, *J. Appl. Meteorol.*, *8*, 799–814, 1969.

Zipser, E. J., Mesoscale and convective-scale downdrafts as distinct components of squall-line structure, *Mon. Weather Rev.*, *105*, 1568–1589, 1977.

Zipser, E. J., and K. R. Lutz, The vertical profile of radar reflectivity of convective cells: A strong indicator of storm intensity and lightning probability, *Mon. Weather Rev.*, *122*, 1751–1759, 33, 1994.

―――――――――

P. Artaxo, A. Plana-Fattori, H. R. Rocha, M. A. F. Silva Dias, and P. L. Silva Dias, Universidade de São Paulo, Rua de Matao 1226, 05508-900, São Paulo, São Paulo, Brazil. (mafdsdia@usp.br)

S. Rutledge, Colorado State University, Fort Collins, CO, USA.

A. J. Dolman and P. Kabat, Alterra, Netherlands.

R .C. S. Alvalá, R. Gielow, A. O. Manzi, J. Marengo, C. Nobre, and L. D. A. Sá, Instituto Nacional de Pesquisas Espaciais, Brazil.
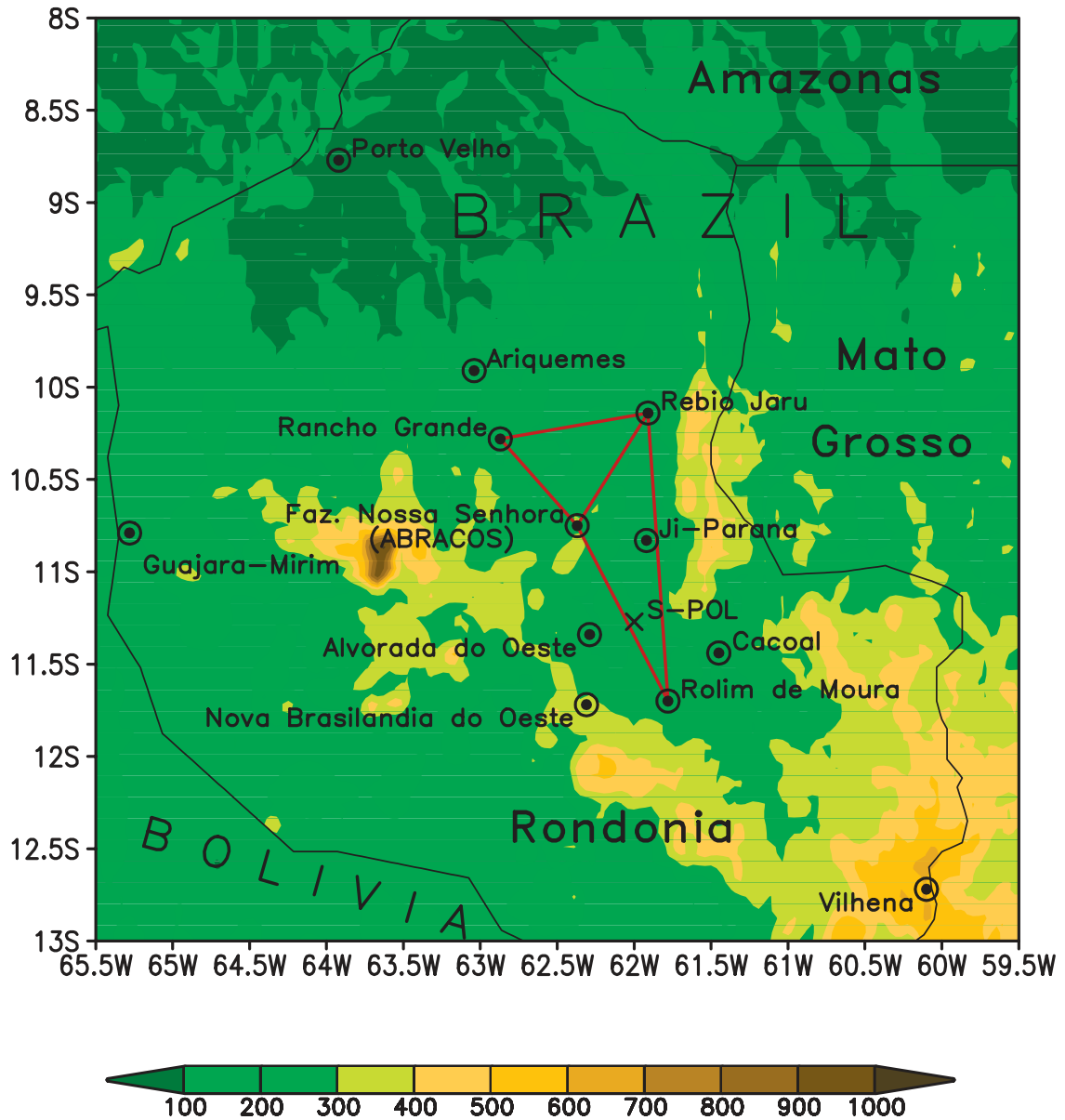
G. Fisch, Centro Tecnológico da Aeronáutica, Brazil.

E. Zipser, University of Utah, Salt Lake City, UT, USA.

J. D. Fuentes and M. Garstang, University of Virginia, Charlottesville, VA, USA.

M. O. Andreae, Max-Plank-Institut fur Chemie, Mainz, Germany.

L. Gatti, Instituto de Pesquisas Energéticas e Nucleares, Brazil.

Figure 2. WETAMC/LBA and TRMM/LBA sites. Shaded in the background is topography with light gray denoting higher terrain.

Figure 3. Deforestation in the background in light green. Dark green is forest. Rain gauge networks in red. Center of the range circles (at every 20 km) is at the S-Pol position in Fazenda Jamaica. Yellow circles are the Dual Doppler regions. TOGA radar position is indicated by T. S-Pol position is indicated by S. Rain gauge networks are indicated by numbers 1, 2, 3, and 4.